END
DATE
FILMED

9 8!

DTIC

Final Technical Report

by

Dr. J.E. Field, Dr. ..., Dr. ...,

and Dr. ...

DECEMBER 1980

EUROPEAN RESEARCH OFFICE
United States Army
London, N.1., England

Contract Number ...

Physics and Chemistry of Solids
Cavendish Laboratory
Cambridge, England

REPORT DOCUMENTATION PAGE

READ INSTRUCTIONS
BEFORE COMPLETING FORM

1. REPORT NUMBER	2. GOVT ACCESSION NO.	3. RECIPIENT'S CATALOG NUMBER
	AD-A103275	

4. TITLE (and Subtitle)	5. TYPE OF REPORT & PERIOD COVERED
DEFORMATION AND THERMAL PROPERTIES OF ENERGETIC MATERIALS	
	6. PERFORMING ORG. REPORT NUMBER

7. AUTHOR(s)	8. CONTRACT OR GRANT NUMBER(s)
J.E. Field, M.M. Chaudhri, G.M. Swalloe and T.B. Tang	DA-ERO-76-G-073

9. PERFORMING ORGANIZATION NAME AND ADDRESS	10. PROGRAM ELEMENT, PROJECT, TASK AREA & WORK UNIT NUMBERS
Physics and Chemistry of Solids Cavendish Laboratory Madingley Road, Cambridge CB3 OHE UK	6.11.02A - 1T161102BH57-08

11. CONTROLLING OFFICE NAME AND ADDRESS	12. REPORT DATE
	December 1980
	13. NUMBER OF PAGES
	53

14. MONITORING AGENCY NAME & ADDRESS(if different from Controlling Office)	15. SECURITY CLASS. (of this report)
	15a. DECLASSIFICATION/DOWNGRADING SCHEDULE

16. DISTRIBUTION STATEMENT (of this Report)

APPROVED FOR PUBLIC RELEASE - Distribution Unlimited

17. DISTRIBUTION STATEMENT (of the abstract entered in Block 20, if different from Report)

18. SUPPLEMENTARY NOTES

19. KEY WORDS (Continue on reverse side if necessary and identify by block number)

Explosives, ignition, impact, sensitiveness, hot spots, high speed photography, decomposition, kinetics, PETN, HMX, polymers, silver azide.

20. ABSTRACT (Continue on reverse side if necessary and identify by block number)

The report covers four areas of work. In the first it is shown that some polymers can sensitise explosives in impact situations. The effect is primarily a mechanical one with the production of free radicals by the polymer only of secondary importance. Chemical effects were assessed using TG. High speed photography, with the sample between transparent anvils, was used to photography impacts on polymers, explosives and layers of explosive with polymers added. Polymers which sensitise are those which fail catastrophically, either by fracture or localised adiabatic shear, and which have a low specific

DD FORM 1473 EDITION OF 1 NOV 65 IS OBSOLETE
1 JAN 73

heat, latent heat and thermal conductivity. Hot spots in these polymers during rapid deformation can greatly exceed the polymers softening point. This was confirmed by separate experiments with a friction apparatus with hot spot temperatures recorded using I.R. techniques. The second study describes a graphical computer method for analysing TG and DSC traces which gives all three reaction parameters (E,A,n) characterising an nth order reaction from a single trace. The final areas of research described are concerned with the analysis of (i) isothermal kinetic data and (ii) dynamic kinetic data from solid-state reactions.

CONTENTS

1. INTRODUCTION

It is now generally accepted that the behaviour of a reactive material needs to be considered in terms of its explosive, its thermal and its mechanical properties. Most explosives deform before initiation and the details of this deformation determine how energy can be localised to give "hot spots". Once heat is produced locally the "hot spot" temperature is controlled by the heat being produced and the flow of heat away from the "hot spot". To understand this process it is important to have the reaction parameters of the explosive and thermal properties such as specific heat and conductivity. For many explosives, particularly new compositions, these are not always known accurately.

The research on this contract has considered the mechanical and thermal properties in some detail. Studies of initiation and propagation have been greatly aided by high-speed photography. Research on reaction kinetics and thermal properties has used mass spectroscopy, differential scanning calorimetry (DSC), thermogravimetric analysis (TG) and scanning electron microscopy. Mechanical properties experiments include measurements of hardness, yield strength, coefficient of friction and fracture surface energy.

The four areas of work described in this report have either been published (sections 2,3,4) or are ready for submission (section 1). The texts of these papers are given in full.

2. THE IGNITION OF A THIN LAYER OF EXPLOSIVE BY IMPACT; THE EFFECT OF ADDED POLYMER PARTICLES. G.M. Swallowe and J.E. Field.

2.1 Introduction

A study of the deformation behaviour of a thin layer of material when impacted is relevant to a range of problems including the sensitiveness of explosives. A standard test procedure for assessing the hazard involved in handling explosive materials is to impact a sample (typically 20-50 mg) with a falling weight. The sensitiveness of a sample is usually expressed in terms of a 50% drop height to cause ignition (i.e. the height from which the weight would ignite 50% of a series of samples). There are standard methods for obtaining the 50% height (see, for example, Dixon and Massey, 1957). However although the test has been used for many decades it is only recently that a systematic attempt has been made to photograph the sample during its deformation (Heavens, 1973, Heavens and Field 1974). A combination of high-speed photography combined with pressure measuring techniques helped establish the physical processes occurring during ignition and propagation.

In general it is thought that the initiation of an explosive by mechanical shock is thermal in origin, although some workers believe that a tribochemical or a molecular fracture mechanism may be responsible in certain circumstances (Taylor and Weale, 1932, Ubbelohde, 1948, Fox, 1970). On the basis of localized thermal energy or "hot spots" as the source of the explosion, four possible mechanisms have been envisaged for ignition by impact.

(i) Adiabatic compression of trapped gas spaces (Bowden, Mulcahy, Vines and Yoffe, 1947, Chaudhri and Field, 1974).
(ii) Viscous heating of material rapidly extruded between the impacting surfaces (Eirich and Tabor 1947, Bolkhovivinov and Pokhil 1958) or by capillary flow between grains (Rideal and Robertson, 1948).

(iii) Friction between the impacting surfaces and/or grit particles and/or grains of the material (Bowden and Gurton, 1949).

(iv) Localised adiabatic deformation of the thin layer upon mechanical failure (Afanas'ev and Bobolev, 1971, Winter and Field, 1975).

It was shown quite convincingly (Bowden et al, 1947) that the presence of gas bubbles affected the impact sensitiveness of nitroglycerine, and Bowden maintained repeatedly (Bowden and Yoffe, 1949, 1952, 1958, Bowden, 1950, 1963) that mechanism (i) was the primary cause of ignition, not only in liquids but also in solid explosives. This view has with equal persistence been rejected by the Russian school of thought (Andreev, Maurina and Rusakova 1955, Bolkhovitinov, 1959, Afanas'ev and Bobolev, 1971). In impact experiments on solid explosive materials it was discovered (Kholevo, 1946) that the sensitiveness was considerably reduced if the sample was prevented from flowing. Afanas'ev and Bobolev (1961) produced evidence from strain-gauge experiments which suggested that during impact the sample suddenly undergoes a type of fracture. These authors proposed a mechanism of hot-spot formation by the release of energy along slip surfaces formed at the onset of mechanical failure (Afanas'ev and Bobolev, 1971, Afanas'ev, Bobolev, Kazarova and Karabanov 1972).

The high-speed camera work of Heavens and Field (1974) showed that impacted samples in the drop-weight test may undergo bulk plastic flow, show evidence of partial fusion and even (with PETN) melt completely. The flow speed during these processes is considerable and may reach a few 100 m s^{-1}. Ignition occurred at a small number of local hot-spots. Strain gauge measurements showed that pressures of typically 0.5 - 1 GPa (5 - 10 kbar) were achieved. If a sample failed by plastic flow this was accompanied by a sharp pressure drop. It was after the pressure drop that the high velocity flow phenomena took place and ignition occurred. Hot-spots were thought to be caused either by local obstructions in the flow or by the rapid closure of gas pockets trapped in the material.

Recent work has been concerned with studying the effect of added grit particles in greater detail. The case of the hard, high melting point particle is reasonably well understood (Bowden and Gurton 1949, Bowden and Yoffe 1952, Ubbelholde 1948). The basic idea is that when two solids rub or impact together the hot-spot temperature at the interface is determined by the solid with the lowest melting point. Properties such as thermal conductivity and hardness are important but only as second-order effects. In fact by chosing grits of different melting point and measuring the impact sensitiveness Bowden and Gurton were able to measure hot-spot ignition temperatures for a range of explosives. The hot-spot temperature found by these workers for PETN in a drop-weight impact situation was ca. 700 K for hot-spots of micron dimensions.

It is now known that certain polymers such as polycarbonate (PC) and polysulphone (PS) can also sensitise explosives in the drop-weight test though others such as polypropylene (PP) do not (Bean 1973). At first sight this result appears surprising since polymers are relatively soft and have softening temperatures usually well below the 700 K mentioned above. The primary object of our new work was to try to understand the mechanisms by which some polymers give increased sensitiveness and why others do not. At the start it appeared possible that the explanation could be a

chemical one based on the production of free radicals which aided the
reaction kinetics of the explosive or a mechanical one in which hot-spots
were produced by the deformation of the polymer. The first experiments
were concerned with possible chemical effects and used techniques such as
differential scanning calorimetry (DSC) and thermogravimetric analysis (TG).
The mechanical effects were studied using the photographic and pressure
measuring techniques described earlier.

2.2 Studies of Chemical Effects

Experimental

These experiments involved measuring the reaction parameters for decom-
position of pure explosive and explosive/polymer mixtures and assessing
any differences. The apparatus used was a Stanton-Redcroft TG-750 thermo-
balance which allows the weight of the sample to be monitored whilst it is
heated at a constant rate, thus giving a weight-loss versus temperature
curve. The samples used consisted of $\sim$ 1 mg lots of a mixture containing
25% (by weight) of polymer to 75% explosive. This percentage of polymer
is much greater than likely to be found in practice, but was chosen to
amplify any interaction. The explosive used in all these experiments was
pentaerythritol tetranitrate (PETN). The analysis follows the method
of Hauser and Field (1978 and section 3 of this report) and so is only
briefly outlined here.

Decomposition is assumed to follow an equation of the form

$$\frac{dw}{dt} = - A \exp(-E/RT)w^n \tag{1}$$

with w the fractional residual weight at time t, E the activation energy,
A the frequency factor, n the reaction order and T the temperature. Since
the heating rate H is constant, one may write $dT/dt = H$. Substituting
in equation 1 and taking logs yields:

$$\ln\frac{dw}{dT} = \ln\frac{A}{H} - \frac{E}{RT} + n \ln w \tag{2}$$

Thus a plot of $(\ln dw/dT - n \ln w)$ against $1/T$ gives a straight line if
n has been chosen correctly. The value of E is determined from the slope
of the line and A from its intercept. The analysis was carried out on the
Cambridge IBM 370/165 computer. The programs used fit a cubic spline to
the original data and produce differentials which are then used to give plots
of $(\ln\frac{dw}{dt} - n \ln w)$ against $1/T$ for values of n from 0 to 2 in steps of 0.2.
The straightest section of these curves for each stage of the reaction
(there may be more than one) was then selected by eye and the appropriate
values of n, E and A obtained. The method is illustrated by the activation
energy plot for a sample of pentaerythritol tetranitrate (PETN) in Figure 1.
The technique was assessed in two ways. Firstly by using the obtained
reaction parameters and simulating a decomposition curve which could be
compared with the original. Secondly, the dehydration of calcium oxalate
monohydrate was observed.

$$CaC_2O_4H_2O \rightarrow CaC_2O_4 + H_2O$$

This reaction is well understood and the reaction parameters are well documented in the literature (Gurrieri, Siracusa, Cali, 1974, Freeman, Carroll, 1958). The results obtained with the technique outlined above were in good agreement with the literature values and are set out in Table 1.

Table 1: Dehydration of Calcium Oxalate Monohydrate

	$E/kJ\ mol^{-1}$	$\ln A/\ln\ s^{-1}$
This work	89.5 ± 3	20.2
Literature	88.6	21.1

Results

(a) Thermal decomposition of PETN/polymer samples

The polymers reported to sensitise PETN (Bean, 1975) were polycarbonate (PC), polysulphone amber (PS) and to a lesser extent polypropylene (PP). Results obtained in this work confirmed the dramatic effect produced by PS and PC but showed very little increased sensitivity in the presence of PP*. Samples of these polymers supplied by AWRE were ground in a freezer mill to sizes of <76 µm and then mixed with PETN to produce experimental samples. The heating rate used throughout was 10 deg min^{-1} and the purger gas nitrogen or argon. The results are summarised in Table 2, the figures listed being averages of between three and seven different experiments.

Table 2: Effect of Polymeric Additives on the Thermal Decomposition of PETN

Sample	$E_s/kJ\ mol^{-1}$	$E_d/kJ\ mol^{-1}$	$\ln A_s/\ln\ s^{-1}$	$\ln A_d/\ln\ s^{-1}$	n	T/K
PETN	143 ± 5	193 ± 7	31 ± 4	44 ± 6	0.7	478
PETN+PC	130 ± 10	214 ± 30	30 ± 6	53 ± 10	1.0	476
PETN+PP	122 ± 15	172 ± 15	28 ± 4	41 ± 6	0.6	477
PETN+PS	130 ± 10	231 ± 20	30 ± 4	49 ± 10	1.0	474

In each case, a two stage reaction was observed (Figure 1), the first stage being identified with the sublimation of PETN (E_s, A_s) and the second its decomposition (E_d, A_d). The values obtained for the activation energies of sublimation (143 ± 5 kJ mol^{-1}) and decomposition (193 ± 7 kJ mol^{-1}) are in good agreement with the literature values. Cundall, Palmer and Wood, (1977) quote 150.4 kJ mol^{-1} for the sublimation of PETN while Roberston (1948), Rogers and Morris (1966) Maycock and Verneker(1970) and Ng, Field and Hauser (1976) give values for the decomposition of 197,198,188 and 192 kJ mol^{-1} respectively. The value for $\ln A_d$ of 43.5 is also in good agreement with the 45.6 reported by Robertson (1948).

A larger spread is observed in the values of E_d in the PETN/additive samples than the pure PETN. However, although some activation energy differences are observed, there are no significant changes or consistent trends. The values of frequency factor are much less accurate than those of activation energy since they have been obtained by measuring the intercept

---

* The sensitising effect reported by Bean for PP in PETN is surprising and we query the effect. It is contrary to our results and in fact Bean's results for PP in other explosives show little or no positive effect.
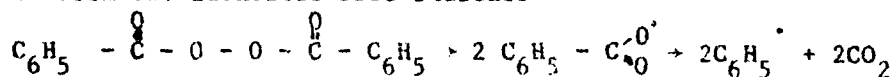
rather than the slope. Again within the errors of measurement, they show no significant changes from the values for pure PETN. If the additive had significantly affected the reaction towards greatly increased reaction rate then A should have increased and E decreased. Table 2 shows that only small changes in A and E took place, and further that any changes of A and E tended to cancel (i.e. as A increases, E also increases and vice versa).

The only consistently observable feature in the results is a change in the value of n from 0.7 to 1.0 (except in the case of PP). A value of n ca. 0.7 implies a surface reaction (for which n = 2/3) and n = 1.0 is the value one would expect for a bulk reaction. The explanation for this is that the high proportion (25%) of filler material distributed throughout the sample breaks up the PETN giving it a greater surface area, thus favouring a bulk rather than a purely surface reaction. The result for PP is explained by the fact that it softens and melts at a lower temperature than the other polymers. PETN/PP samples were observed to give droplets of polymer which then coalesced to form one drop. This effectively removed the dispersion of particles which gives n approaching unity leaving a surface reaction with n ca. 2/3.

(b) Thermal decomposition of PETN/Benzoyl peroxide samples

The results of the preceeding section show that the additives tested have very little effect on the thermal decomposition of PETN. It may, therefore be concluded that their sensitising effect is not due to polymer decomposition products interacting with PETN. However, the possibility still exists that, when polymers fracture or flow during impact, large concentrations of free radicals may be produced, and these could react with PETN and cause ignition.   Walker and Green (1976) have proposed that the mechanical production of free radicals is important in initiation and have done some experiments in which they find that tetramethylammonium tribohydride (a free radical donor) causes increased reaction with ammonium nitrate.

In order to test this hypothesis, mixtures of benzoyl peroxide and PETN were used in a series of TG experiments. Benzoyl peroxide is an organic oxide which thermally breaks down in the temperature range 310 to 350 K to form two identical free radicals

$$C_6H_5 - \overset{O}{\underset{}{C}} - O - O - \overset{O}{\underset{}{C}} - C_6H_5 \rightarrow 2\ C_6H_5 - C\overset{O^\cdot}{\underset{O}{\diagdown}} \rightarrow 2C_6H_5^\cdot + 2CO_2$$

It is widely used in the polymer industry as a 'starter' material for free radical polymerisation as it provides a good source of easily formed free radicals.

A number of TG runs were carried out on both benzoyl peroxide by itself and two PETN/benzoyl peroxide mixtures. The mixtures used had compositions of 75% to 25% and 93% to 7% by weight of PETN/benzoyl peroxide.

Due to the decomposition of the benzoyl peroxide, the only activation energy that can be estimated is the decomposition of PETN, the sublimation stage being buried in the benzoyl peroxide reaction. Simulated computer decompositions of these mixtures were made by combining 75% of the numerical value of pure PETN run with 25% of the numerical value of a pure benzoyl peroxide run (and similarly for the 93/7 mix). The figures thus obtained

were treated as if they had been real data and the analysis carried out in the usual manner. Comparison of the E,A and n values obtained in real and simulated experiments, Table 3, reveals that what appears at first to be a very strong chemical interaction is due to the combined effects of the two materials acting independently.

Table 3: Reaction Parameters for PETN/Benzoyl Peroxide (b.p.) Sam

Sample	$E_d/kJ\ mol^{-1}$	$\ln A_d/\ln S^{-1}$	n
7% b.p. 93% PETN	185 ± 8	46 ± 2	0.7
7% b.p. 93% PETN (Simulation)	176 ± 16	41 ± 5	2/3
25% b.p. 75% PETN	120 ± 6	29 ± 2	0.6
25% b.p. 75% PETN (Simulation)	143 ± 20	33 ± 2	2/3

(c) Effect of ultra-violet light on the thermal decomposition of PETN/grit samples

As a further test of the free-radical initiation hypothesis, PETN/additive samples were irradiated with ultra-violet light as they were being heated in the TC. U-V is frequently effective in degrading polymers by breaking chains with the formation of free radicals. Both PP and PS are susceptible to photodegradation by U-V whereas PC is degraded relatively much less. It would therefore be expected that, if free radicals are important in sensitising PETN, both PP and PS in combination with U-V should show an appreciable effect and PC little or no effect. The results obtained in these experiments are set out in Table 4.

Table 4: Reaction Parameters in the Presence of U-V Light

Sample	$E_s/kJ\ mol^{-1}$	$\ln A_s/\ln s^{-1}$	$E_d/kJ\ mol^{-1}$	$\ln A_d/\ln S^{-1}$	n	T_p/K
PETN	143 ± 5	31 ± 4	193 ± 7	44 ± 6	0.7	478
PETN + U-V	120 ± 4	28 ± 2	183 ± 16	45 ± 4.5	0.6	458
PETN + U-V + PC	124 ± 8	29 ± 3	196 ± 25	49 ± 7	0.9	458
PETN + U-V + PP	102 ± 8	22 ± 4	186 ± 8	45 ± 3	0.6	458
PETN + U-V + PS	112 ± 8	25 ± 2.5	$E_{d_1} 368 \pm 9\ \ln A_{d_1} 99 \pm 6$ $E_{d_2} 185 \pm 15\ \ln A_{d_2} 47 \pm 5$		1.4	446

Except for the rather anomalous behaviour of PS in the decomposition stage (see later), the results indicate that only small effects are produced.

The changes in the sublimation parameters E_s and A_s tend to cancel in all cases and for the decomposition parameters E_d and A_d changes again effectively compensate, particularly for polycarbonate. PP, PS and pure PETN all show decreases in E_d (E_{d_2} in the case of PS) combined with increases in A_d (A_{d_2} with PS). Thus the reaction is helped, albeit a little, by the U-V radiation. This is illustrated by the slight but consistent, reduction in the reaction peak temperatures T_p.

PS shows the most significant changes in that an extra reaction stage appears. This result was found to be very repeatable, though it is not fully understood. Although E_{d_1} (for the new stage) is very high, the value of A_{d_1} more than compensates for this, and T_p is reduced by 12 K. The initial and final stages of the reaction are virtually unchanged by the presence of this new stage, which only has a small (ca. 9 K) range of activity.

A further series of experiments on the PETN/PS system was carried out in which the U-V light was switched on or off during the course of a run and the effect on the reaction parameters noted. These experiments show that the stage of reaction at which the U-V is present is quite important. If the U-V is switched on at any stage before a third of the material present has decomposed, then a three stage reaction is observed, otherwise no effect is observed. When U-V has been present for the initial stages of the reaction (even if only one eighth of the explosive has decomposed) extinguishing the light has no effect and the reaction proceeds in three stages, as if the U-V were present throughout.

These results indicate that the U-V is effective in breaking down the PS to produce free radicals which then influence the decomposition of PETN. If, however, PETN decomposition has proceeded to a significant extent before the U-V is present, the irradiation has little effect. This is probably because the free radical concentration produced by the PETN alone is already much greater than that which the lamp can produce. The observation that extinguishing the lamp early in the reaction does not stop the three stage process indicates that the major influence is the concentration of free radicals in the initial stages of decomposition. The influence of U-V may thus be summarised as producing such a concentration of radicals in the early stages of PETN decomposition that the decomposition process is speeded up and the reaction parameters (and presumably the details of the mechanism) are changed.

That PC is not influenced in this way is not surprising since, in comparison with other polymers, polycarbonates are not degraded to any large extent by U-V (Ranby and Rabak, 1975). It is, however, surprising that if such an effect should be produced with PS,PP remains ineffecitve. Both PS and PP are degraded to a large extent by U-V and both produce large concentrations of radicals when degraded. It suggests that the sulphone groups have a specific effect on at least one of the stages of the PETN decomposition. Support for this comes from the work of Reich (1973) who tested the compatibility of a range of polymers with various explosives. PS is one of the polymers he lists as incompatible with PETN since he detected an increase in the value of the reaction parameter n in the present of PS.

From the series of experiments described in this section, it may be concluded that there is no major chemical reaction between PETN and any of the polymer fillers. The only exception to this is PS and then only in the extreme conditions of having a high intensity of U-V shone on the sample. However, the effect, even with PS, is still only marginal and the conclusion has to be that chemical effects, although present, are only of secondary importance compared with the mechanical ones to be discussed in the following section.

2.3 Photographic Observations of the Impact Behaviour of Polymers and Explosives

(a) High-speed photography of impacts on polymer samples

The impact behaviour of both polymers and explosives was photographed using a C4 rotating mirror framing camera at framing intervals of ca. 6.5 μs. Impacts were observed using a transparent toughened glass anvil system similar to that of Heavens and Field (1974) and is shown schematically in Figure 2. The weight of 5.5 kg was dropped by an electromagnet from a height of 1 m, the fall being guided by three cylindrical rods.

The behaviour of small discs of polymer ca. 2 mm diameter and 0.8 mm height under impact is illustrated in Figure 3. Figure 3 shows selected frames from an impact on a disc of PP. A trace of radial expansion versus time is given in Figure 5. With this material, there are no rapid changes in the expansion rate and bulk deformation occurs throughout. Figure 4 is a higher magnification sequence for an initially 2 mm diameter disc of PS. Its radial expansion is also included in Figure 5. This material deforms initially in a bulk manner but eventually fails catastrophically (see frame 4(c) and Figure 5). PC gives similar catastrophic failure to PS. Microscopic examination of the samples after impact confirms that catastrophic failure of PC and PS is associated with rapid cracking and shearing in localised bands. Figure 6 is a micrograph of a deformed PS disc. There is a network of fracture throughout the sample and sets of fine parallel shear bands (one set is labelled s). An enlarged view of region s, but rotated so that the bands are horizontal in the figure is given in 6b. It is argued later that it is these regions of localised deformation (cracking and shear banding) which give rise to "hot-spots".

These observations lead to the conclusion that the polymers used may be classified in two broad groups: (i) Polymers such as PC and PS which fail by the production of many fast moving cracks and local shear bands. This is accompanied by rapid radial expansion. (ii) Polymers such as PP which deform plastically at quite a high rate but do so by bulk deformation and without cracking and/or shear banding.

(b) High-speed photography of impacts on explosives

Heavens and Field (1974) photographed the impact of a wide range

of granular explosives.   Powdered PETN was observed to be compacted into
a pellet and then to undergo severe plastic deformation.   The material
became translucent and finally completely transparent with very rapid flow
(300 m s⁻¹) which Heavens and Field attributed to melting.   Ignition occurred
in this final stage.   RDX partially fused when impacted between glass anvils
and there was indirect evidence of complete sample melting of RDX between
steel anvils.   Pressure-time curves obtained by Heavens and Field showed
that a sharp pressure drop occurred when the sample failed plastically.
Ignition, in samples without added grit particles, always occurred after
the pressure drop and when the explosive was flowing rapidly.   In the
present work a large number of experiments were carried out on pellets of
PETN and the behaviour was very similar to that described by Heavens
and Field for granular material.   Figure 7 illustrates a typical
result in which a 25 mm pellet of PETN, pressed to 5k bar and of diameter
5 mm is impacted by a 5.5 kg mass from a height of 1 m.   The same type of
behaviour as described for powders, can clearly be observed.   In frames
a to f the material is deformed plastically and becomes translucent.   Trans-
parency and rapid flow (230 m s⁻¹) occur in frame g with ignition at sites A
and B almost simultaneously.

The results obtained with a large number of such sequences show that
ignition   only occurs if rapid flow, as observed in frame g, takes place.
Although rapid flow is a necessary prerequisite for ignition   the converse
is not necessarily true and many failures occur without a resulting ignition
This suggests that there has to be a particular region in the flowing material
where a "hot-spot" develops.   These regions could be associated with gas
bubbles, foreign particles or enhanced flow.   If discontinuities of sufficient
size do not exist, ignition   does not take place.   Note that fast reaction
always starts at localised regions (see Figure 7 and the sequences in
Heavens and Field).

(c) High-speed photography of impacts on explosive/polymer samples

A number of high-speed photographic sequences at framing rates of up
to 2×10^5 frames per second have been taken of impacts on explosive/grit
samples.   These sequences were taken in transmitted light using the experi-
mental set-up described above.   The first point to emerge from these
experiments was that, unlike impacts on pure PETN where ignition   never
occurs before transparency and rapid flow of the sample, have occurred,
when a grit is present, ignition can take place before the explosive has
been sufficiently compacted to fail plastically, form a transparent layer
etc.   This observation implies that the pressures needed to cause explosion
are much smaller than with a pure material.

If a sample ignites while it is still opaque it means that small
polymer particles within the pellet can not be seen, and thus association
of the initiation sites and grit particles is difficult.   To overcome this
problem, two different approaches were adopted.   In the first instance,
pressed pellets of pure explosive were surrounded by polymer discs and the
impact phenomena of the whole array photographed.   The second type of experi-
ment involved pressing pellets of explosive, into which had been put single
polymer discs, effectively modelling a single large polymer particle in a
sample of pure explosive.   Examples of results obtained from these experi-
ments are illustrated in Figures 8-11.

Figure 8 shows a 0.65 mm high PETN pellet surrounded by five 1 mm
high PS discs.   During the impact the PETN disc (dark central area) breaks
up and is forced into close contact with the polymer.   The polymer discs
deform plastically and then undergo catastrophic failure as described
earlier.   In frame 8b all the discs are exhibiting cracking and shear band-

ing and by frame 8c have failed catastrophically.   In frame 8d we can
see the first ignition site (labelled 1) with reaction spreading along
two paths into the PETN.   A second site (labelled 2) has developed in
frame 8e.   By the final frame, fast reaction has spread throughout most
of the PETN.

An example from the second type of experiment is shown in Figure 9.
In this case a single polymer disc of PS was pressed with the PETN
powder to form a composite disc.   The selected frame shows ignition at
three points (1 to 3) on the polymer/explosive interface.   The polymer
is the lighter central area, and the darker annulus is the PETN.   In
the lower part the PETN is becoming lighter and this is due to the onset
of fusion.   At its outer edge the PETN is beginning to produce fast jets.
The mottled appearance of the polymer is partly due to catastrophic failure
and partly due to a very thin layer of trapped PETN.   This is why reaction
also spreads inwards as well as outwards.   Frame 9b shows a later state
where fast reaction is more developed.   The expansion velocity of the PS
disc just prior to ignition was ca. 35 m s^{-1}.   The catastrophic failure
occurred between frames.   Experiments with PC showed that it behaved
in a very similar manner, with cracking and rapid radial expansion followed
by ignition at the interface.

The situation with PP is quite different and, although much radial
expansion at quite high velocities is observed, the polymer does not crack
or shear locally and ignition does not occur.

The results obtained with HMX/polymer systems are similar to those
obtained with PETN.   Figure 10 illustrates an impact on a 20 mg sample
containing a PP disc and Figure 11 a 20 mg sample containing a PC disc.
In both cases the polymer is the light central area and the explosive the
darker area.   Figure 10 shows that yield and flow of both the PP and HMX
occur but no ignition results.   In Figure 11 ignition occurs at the polymer/
HMX interface (frames d onwards) after catastrophic failure of the PC.

The findings of the photographic work described in this section may
be summarised as: (i) ignition occurs after or during the catastrophic
failure, cracking and fast flow of the polymer; (ii) the initiation site
is very closely associated with the position of the polymer and (iii) of
the polymers tested, only those which undergo catastrophic failure are
effective in promoting ignition.

2.2   Impact Behaviour in the Drop-Weight Test

(a)   Impacts of polymer samples

Samples of the polymeric materials were impacted in a drop-weight
machine at strain rates similar to those observed in the photographic
work ($\dot{\varepsilon}$ ca. 10^3 s^{-1}) so that differences in their mechanical behaviour
could be observed.   The drop-weight machine used was similar to that des-
cribed by Heavens and Field (1974) and is illustrated schematically in
Figure 12.   The sample was placed between rollers R1 and R2 which had their
edges ground down to give a sharply defined contact area of diameter 5 mm.
The samples used were discs of polymer typically 1.5 mm high and 7 mm dia-
meter.   The contact area was lubricated with colloidal graphite.   Two
semiconductor strain gauges were mounted in series diametrically opposite
to each other on R3 in order that the resistance change induced in the
pair of gauges during impact would be due to compressive stresses alone.

The system was calibrated statically using an Instron machine.

As the sample diameter was greater than the contact area, the area of contact during impact remained constant throughout the whole process. The pressure-time traces were obtained on paper-tape utilising a Data Lab DL922 transient recorder and analysed on a HP9825 calculator using a programme based on the method of analysis of Afanas'ev and Bobolev (1971). The programme numerically integrates the force-time trace produced by the .equipment to yield a velotiy-time trace for the weight

$$V(t) = V_0 - M^{-1} \int_0^t F(t) \, dt \qquad (3)$$

with V_0 the velocity of the weight at impact and M its mass. A second integration gives the displacement of the weight as a function of time $z(t)$.

$$z(t) = \int_0^t V(t) \, dt \qquad (4)$$

$z(t)$ is the compression of the whole system (sample and anvils) and a small amount $z_a(t)$ due to the compression of the system, which can be determined by performing impact with no sample present, is subtracted from $z(t)$ to yield the compression of the sample.

$$z_s(t) = z(t) - z_A(t) \qquad (5)$$

The sample strain is then given by

$$\varepsilon(t) = \ln \left(\frac{H}{H - z_s(t)} \right) \qquad (6)$$

with H the initial height of the sample and $\varepsilon(t)$ the strain at time t. The stress at time t is given by division of the force-time curve by the area of contact A.

$$\sigma(t) = F(t)/A$$

Elimination of t between equations 5 and 6 yields the stress-strain curve.

Results obtained with PC and PP are illustrated in Figure 13 (a) and (b). The behaviour of PS was similar to that of PC. The main difference between the two materials is the evidence of catastrophic failure in PC (as shown by the sharp drop at $\varepsilon = 1.8$) and its absence in PP. Both materials show evidence of strain softening followed by orientation hardening, but the strains which PP is capable of are far greater than those achieved by PC. The onset of orientation hardening also takes place much earlier in PC at a strain of ca. 0.5 as opposed to the value of 2.0 observed with PP. At strains of >2 the thickness of the PP layer becomes comparable to the correction factor for anvil deflection and thus the calculated strain become increasingly unreliable.
The shape of the stress-strain curve may therefore be inaccurate at high strains These results confirm the findings of the photographic work in showing a marked difference in high strain rate impact behaviour between sensitising and non-sensitising materials and again point to catastrophic failure as being the process responsible for a polymer's sensitising action.

(b)   Impact behaviour of explosive/polymer samples

The sensitivity of pure explosives PETN and HMX and explosive/polymer samples were compared by determining their 50% height on the drop-weight machine outlined above. The 50% height is the height from which the hammer, if allowed to fall freely, would have a 50% probability of causing initiation. The method of determination was based on the "up and down" method which is fully described in Dixon and Massey (1957).

A large number of drop-weight tests were carried out on explosive/grit samples to determine (i) which polymers gave rise to increased sensitiveness, (ii)if the size of the grit particles was important,(iii) the effect of variation of the percentage weight of grit, and (iv) if a polymer which sensitised one secondary was effective in sensitising another. All the experiments were carried out using twenty 25 ± 1 mg samples of powder which had been pressed statically to 10 kbar to give pellets of 5 mm diameter and approximately 0.8 mm height. In these experiments, three grades of grit were used which have been called coarse, fine and very fine. In the 'very fine' grade, all the particles had been through a 76 μm mesh, the 'fine' grade indicates that the grit was used as obtained from the freezer-mill with a maximum particle mass of ca. 20 μg. The coarse material was as-received grit from AWRE with particles of mass up to 1 mg and up to 1 mm long. These reuslts are set out in Table 5. Unless otherwise stated, all the samples contained 20% by weight of grit

Table 5: 50% Heights for Explosives and Explosive/Binder Samples

Sample	50% ht (cm)
PETN (pure)	21.8 ± 1.0
PETN + PC (very fine)	10.5 ± 2.0
PETN + PC (very fine) repeat	10.7 ± 0.6
PETN + PS (very fine)	11.1 ± 0.3
PETN + PS (fine)	13.0 ± 1.5
PETN + PS (coarse)	10.4 ± 0.6
PETN + PS (1 mm high, 1mm diam.)	10.5 ± 3.0
PETN + PMMA (coarse)	21.0 ± 1.6
PETN + PMMA (fine)	19.2 ± 0.8
PETN + PP (very fine)	18.8 ± 0.8
PETN + PP (very fine) 10% grit	19.2 ± 0.7
HMX (pure)	29.0 ± 2.0
HMX + PC (fine)	16.0 ± 1.5
HMX + PS (very fine)	15.1 ± 1.0
HMX + PMMA (coarse)	22.6 ± 1.0
HMX + PP (fine)	24.4 ± 0.8
AgN_3 (pure)	19.3 ± 0.8
AgN_3 + PC (fine)	16.8 ± 1.3

From the results set out, it can be seen that the size of the grits used does not have any great effect on the results produced. It might be expected that, if the effectiveness of the grit depended on its ability to disturb the flow of the explosive as it was extruded from between the anvils, the larger particles by virtue of their size would prove more effective, the very fine particles being so small as to be carried along in the flow of the explosive. The results obtained show that this is not a major factor.

The results also show that the grits are not specific in their action: PC and PS being equally effective in sensitising HMX and PETN, while PP and PMMA only slightly sensitise both of these secondary explosives. As noted before (see for example, Heavens, 1973, and Heavens and Field, 1974) primary explosives such as lead azide $Pb(N_3)_2$ and silver azide AgN_3 are not particularly sensitive in the drop-weight test provided the anvils are well-aligned. However, as the table shows, the polymers do have a significant effect on the sensitiveness of AgN_3 and in a consistent way. Finally, in one set of experiments the percentage of grit was reduced to 10% but this caused no significant change.

2. Thermal Properties

(a) Mechanical effects and thermal properties

The mechanical failure properties of polymer additives appear to be of major importance in determining their sensitising effect. Those materials which undergo bulk plastic deformation proving ineffective as sensitisers and those which fail catastrophically and with intense local deformation effective. Thermal properties are of major significance in determining the failure modes of polymers particularly when high strain rates are involved. This is because they soften at relatively low temperatures and have low densities, specific heats and thermal conductivities. Additionally, materials can desensitise explosives by effectively acting as heat sinks and quenching hot spots before they can fully develop. The work of Bowers, Romans and Zisman (1973) for example, indicates that sensitivity decreases with increasing specific heat of additive, those additives which are most effective in this respect being materials such as "Superla wax"or"Carbowax" which have low melting points and thus absorb their heat of fusion.

In cases where thermal properties were not known they were measured using a Perkin-Elmer DSC-2 calorimeter.

The results obtained show that both PC and PS have specific heats which range from 1.25 kJ kg^{-1} K^{-1} at room temperature to 2.35 kJ kg^{-1} K^{-1} at 600 K, the increase being reasonably linear. PC has a melting point of 420 to 430 K which only introduces a very slight increase in the effective specific heat, giving a latent heat of fusion of ca. 7.2 kJ kg^{-1}. PS shows melting over the range 470-500 K with a heat of fusion of ca. 6.6 kJ kg^{-1}. PP has a greater specific heat, varying from 1.92 kJ kg^{-1} K^{-1} at room temperature to 2.09 kJ kg^{-1} K^{-1} at 450 K. It melted over the range 390 - 460 K with a latent heat of fusion of ca. 64.0 kJ kg^{-1} K^{-1}. PMMA had a relatively constant specific heat of 2.9 kJ kg^{-1} K^{-1} over the range 470 - 630 K where a large decomposition endotherm was produced. From the results set out above, it could be predicted that, on the basis of thermal properties alone, the order for hot-spot quenching for the polymers investigated would be PP, PMMA, PC, PS.

Table 6: Physical Properties of Experimental Materials

* Denotes measurements made in this work

MATERIAL	DENSITY g cm^{-3}	ROOM TEMP. SPECIFIC HEAT J g^{-1} K^{-1}	THERMAL CONDUCTIVITY W m^{-1} K^{-1} x 10^{-2}	LATENT HEAT OF FUSION kJ kg^{-1}	SOFTENING OR MELTING POINT K
PETN	1.773	*1.09		*144.7	*414
β HMX	1.96	1.25			555
PP	0.9	*1.92	0.14	*64.0	*390
PC	1.2	*1.25	0.19	*7.2	*420
PS	1.24	*1.25	0.18	*6.6	*470
PMMA	1.19	*2.9	0.17 – 0.25	decomposes	decomposes
HDPE	0.94 – 0.97	2.2 – 2.3	0.45 – 0.52	~270	~400
Polyester	1.21	1.0	0.2		

MATERIAL	GLASS TRANSITION TEMP. K	PLASTIC MODULUS MN m^{-2} x 10^{-2}	MAX ELONGATION IN TENSION %	TENSILE STRENGTH MN m^{-2}	HARDNESS Rockwell; R,M. Vickers; V.
PETN		1.37×10^2			V. 17.9
β HMX		3.1×10^2			V. 40.3
PP	255	8.9 – 13.8	50 – 600	28 – 36	~R95
PC	418	22	60 – 100	52 – 62	~R118
PS	463	24	50 – 100	63	~R120
PMMA	378	25 – 35	2 – 10	45 – 72	~M100
HDPE	~193	5.5 – 10.	50 – 600	20 – 36	R30 – R50
Polyester		40	2	55	M110

Measurements were also made on the specific heat and latent heat of fusion of PETN. It was found that specific heat remained almost constant at 1.09 kJ kg^{-1} up to the melting temperature of 414 K. The latent heat was determined to be 144.7 kJ kg^{-1} with decomposition occurring rapidly after melting. A summary of the thermal properties of the polymers and explosives used in this work is given in Table 6.

2.6 Polymer Friction Experiments

The purpose of the experiments described in this section was to measure the temperatures that a polymer reaches during deformation. In order to do this, a friction machine was constructed which allows the rubbing polymer interface to be viewed by an infra-red detector. Friction cannot be regarded as just a surface shearing effect since, if one of the materials is harder than the other, the asperities on the harder surface can plough out the softer material to an appreciable depth below the surface. It is thus possible for considerably and varied deformations to take place in a frictional situation, and estimates of the surface temperatures achieved are of interest both to the present investigation and the subject of polymer friction and wear in general.

(a) Apparatus and technique

The apparatus constructed to perform these experiments was basically a modification of that described by Bowden and Thomas (1954) and is shown schematically in Figure 14. It consisted of a 50 mm diameter rotating sapphire disc (infra-red transmitting to ca. 5.3 μm) against which a polymer pin was loaded by means of a balance arm. The area of the interface under observation was defined by a 0.8 mm slit mounted directly above the rotating disc. The disc rotated at a frequency of ca. 56 Hz giving an interfacial velocity of ca. 7 m s^{-1}. Above this disc was a PMMA chopper with radial regions in the sequence, blacked-out, slit, PMMA, slit, blacked out etc. The disc was rotated so that the radiation from the interface was chopped at a frequency of 10 kHz. This allowed temperature variations of duration 1 ms or greater to be followed (since, for any one temperature determination, a complete blacked-out to blacked-out sequence must be obtained, i.e. 5 'chops'). After chopping, the radiation was detected by a Mullard RPY 36 infra-red detector which is sensitive over the range 1 - 5.5 μm with a sharp cut-off at 5.5 μm. The detector was biased to give the best signal-to-noise ratio. The detector output was taken to a Tektronix 7A22 amplifier and the amplifier output was fed to a Datalab DL922 transient recorder. Traces were then punched onto paper-tape for analysis on the Hewlett-Packard HP 9825 desk-top calculator and plotter.

The purpose of the PMMA filters was to provide an absorption band (ca. 3.5 μm) which would absorb a differing proportion of the signal depending on the temperature of the source. Thus, by calculating the ratios I/I_F (with I the intensity through the slit and I_F through the filter) for sources of various known temperatures, a calibration curve of I/I_F against temperature could be drawn and estimates of temperatures of other sources made using the curve. In order for the calibration to be valid, it was assumed that the sources (calibration and specimen) were behaving as black-bodies. Problems associated with different substances having differing black-body emissivities are eliminated by the use of the ratio I/I_F.

(b) Calibration

The theory of calibration follows the treatment of Land (1944) and Parker and Marshall (1948). From Planck's radiation law we have

$$E_{\lambda,T} = C \, \epsilon_\lambda \, \lambda^{-5} / (e^{B/\lambda T} - 1) \tag{7}$$

with $E_{\lambda,T}$ the energy emitted by the black-body at wavelength λ and temperature T, C and B constants and ϵ_λ the emissivity of the surface at wavelength λ. This can be approximated to Wien's formula.

$$E = A \, G \, \epsilon_{\lambda_p} \, t \, \lambda_p^{-5} \, \exp(-B/\lambda_p T) \tag{8}$$

with E the radiant energy received by the detector, A a constant dependent on the area of the source, G a constant dependent on the geometry of the system, t the transmission coefficient of the sapphire and λ_p the effective wavelength of response of the detector. The relation between the response of the detector H and the energy falling on it is of the form

$$H = E^m \tag{9}$$

with m a constant.

Thus from equations 8 and 9:

$$\ln H = m(\ln (A \, G \, t) + \ln(\epsilon_{\lambda_p} \, \lambda_p^{-5}) - B/\lambda_p T) \tag{10}$$

When the radiation passes through the PMMA filter the optical properties of the system are changed (I, E, λ and λ_p change) but the factors A, G and t remain the same. Thus if H'^{P} is the reduced output on passing through the filter we may write

$$\ln H' = m(\ln(AGt) + \ln(\epsilon'_{\lambda_p} \, \lambda_p'^{-5}) - B/\lambda_p'T) \tag{11}$$

From equations 10 and 11

$$\ln \frac{H}{H'} = m \left\{ \ln \left(\frac{\epsilon_{\lambda_p}}{\epsilon'_{\lambda_p}} \frac{\lambda_p'^{5}}{\lambda_p^{5}} \right) - \frac{B}{T} \left(\frac{1}{\lambda_p} - \frac{1}{\lambda_p'} \right) \right\} \tag{12}$$

This relation is independent of the source area and geometrical fractors and is independent of the absolute values of the emissivities. It depends only on the differences in optical properties of λ_p and λ_p' (and this is dependent only on the properties of the system with and without the filter). Thus a plot of $\ln\frac{H}{H'}$ against $\frac{1}{T}$ should give a straight line and, in fact, this is what is found.

Initially calibration was carried out using a 2.5 mm thick PMMA chopper disc and a 0.27 mm diameter platinum wire as an artificial hot-spot. The temperature of the wire was varied by changing the DC current flowing through it. The voltage across a central portion of the wire was monitored via two 25.4 μm diameter platinum wires which were spot-welded to the larger wire 48.0 mm apart. These wires were thin enough not to affect the temperature of the larger wire which was considered to be uniform over the 48.0 mm long middle portion. From the knowledge of the resistance of this central portion, its temperature was determined using standard tables. The central portion was

viewed by the detector though a slit of width 1 mm mounted perpendicular to
the length of the wire. Although this gave a good linear relationship over
the range 770 -1270 °C (Figure 15a), the ratios $\frac{H}{H'}$ for lower temperatures
became to high to be measured accurately and errors associated with
the determination of current and voltage across the wire became significant
so a different approach was adopted for the low temperature calibration
of the system.

The thickness of the PMMA chopper was reduced to 1 mm in an attempt to
improve the ratio $\frac{H}{H'}$, and a variable temperature soldering iron, to the tip of
which was attached a thermocouple, was used as the source. The calibration
produced is illustrated in Figure 15(b). A good linear relationship is again
obtained until the temperature drops below ca. 500 K ($\frac{1}{T}$ = 2.1 x 10^{-3}) when
the scatter in the results begins to get quite considerable. This is because
the ratio has again increased to values where the accuracy in its determination
is reduced by noise. At such low temperatures, the power emitted by a source
which is in the range detectable by the detector is very low and considerations
of signal-to-noise ratio is to increase the size of the source. A simple method
of improving the signal to noise ratio is to increase the size of the source.
This has been tried but there are problems associated with doing so which will be
described below. Further reduction in the thickness of the PMMA filter
would improve the ratio $\frac{H}{H'}$, however 1 mm is the smallest commercially
available thickness and it would be necessary to use other materials to
improve the system in this manner. In fact, 0.2 mm thick acetate sheet was
tried but was found to be unsuitable as the position of its absorption bands
was such that very little change in the value of H' was produced for a wide
range (400-600 K) in T.

The calibration was checked by measuring the radiation received from a
thermometer bulb placed beneath a sapphire disc. The bulb was heated by a
soldering iron and, with the iron removed, a temperature reading was taken,
and the result obtained from the infra-red system and the thermometer scale
compared. For a thermometer reading of 488 K, the infra-red system gave a
value of 489 K. For 453 K the system gave 438 K and for the low temperature
of 383 K the system gave 418 K. It can thus be seen, and it is clear from
the calibration curve, that the determination of temperatures below ca. 500 K
leads to an increasing inaccuracy in the result. In the results quoted later
the error in the result is estimated by drawing an envelope which encloses
all the calibration points for values of $\frac{1}{T}$ less than 2.1 x 10^{-3} (dotted
in Figure 15b). The value of 489 K for an 'actual' temperature of 488 K may
be rather fortuitously close and all estimates of temperature will have an
error of the order of $\pm$ 10 K.

The preliminary analysis of the results was carried out by the HP 9825
calculator. A programme to perform this analysis was written which changed the
zero level of the traces such that it intersected the peak-to-peak levels
approximately half-way (see Figure 16). The heights of the peaks were then
deduced by finding the half-way points between the intercepts of the trace and
the axis, taking as the numerical value of the peak height an average of seven
points around (and including) this half-way value. The trace was then plotted
out together with a listing of the peak heights and the remainder of the ana-
lysis (finding the ratio $\frac{H}{H'}$, was done by hand). Figure 16 shows three typical
results. (i) is for a soldering iron at 575 K (ii) for a small diameter PC pin
and (iii) for a large diameter PC pin. The improvement in signal-to-noise ratio
with a larger diameter pin is clear from a comparison of (ii) and (iii) both
of which give approximately the same minimum value of the ratio $\frac{H}{H'}$.

(c) Results

In the experimental investigation, polymer pins of two different diameters were used: small pins of diameter ca. 1.5 mm and larger pins of diameter ca. 6 mm. The smaller diameter pins were used in the initial experiments but for the later measurements large pins were used since the smaller pins gave a poor signal-to-signal noise ratio and were very easily deformed due to their large length/diameter ratio. The main problem with the use of the larger pins was that considerable heating of the sapphire disc took place and surface temperatures of up to 360 K were recorded on placing a thermocouple in contact with the disc immediately (1 - 2 s) after doing a run. Due to the considerable thermal mass of the disc, its rate of cooling was quite slow (10 - 20 degrees per minute) and so the figure quoted above gives a good indication of the bulk temperature reached by the sapphire in the course of an experiment.

An experiment in which the signal level was recorded with the large pin in contact with the disc and again immediately after its removal indicated that the energy due to the bulk heating of the disc accounted for approximately one third of the total signal. Such a large contribution from a lower temperature source will give a mixed signal which will tend to reduce the measured black-body temperature to a value near the mean. Thus the readings obtained with the larger pins will probably be underestimates of the interface temperature. In the table of results given below (Table 7) the maximum black-body temperature recorded by the system for any given polymer, irrespective of the type of pin used is quoted.

The results will, of course, be averages over the total portion of the interface area within the detector's field of view and it is quite likely that some regions (those being highly deformed) will have temperatures above this average value and others will have lower values. By far the largest amount of experimental time was spent on the polymers PP and PC so that with an increased amount of observation time it may be possible to record higher maximum values of temperature for the three other materials. It is, however, interesting that the temperatures obtained follow the order obtained for the sensitiveness of the polymer/explosive mixtures. It is also clear, particularly in the case of PC, that temperatures well above the commercially quoted softening temperature of 410 K and the observed 'melting' temperature (in previous work) of 430 K are obtainable. In the case of PP however this was not found to be the case and no temperatures above the commencement of melting at 390 K were obtained.

Table 7: Temperatures Achieved During Polymer Friction

Polymer	Maximum Interfacial Temperature/K
PP	360 ± 30
PMMA	420 ± 30
PS	450 ± 20
PC	490 ± 10

Examination of the polymer pins after the frictional experiments reveal
that in the case of PC and PS severe deformation of the polymer had been
produced with evidence of much stretching and shearing of molecular layers.
The PP pin, however, present a much more rounded appearance which indicated
that melting of the surface layers had taken place.

Figure 17 shows the overall appearance of the pins after the experiments
(a) is a PC pin and the many layers which have sheared off and built up on
the trailing edge are clearly visible. (b) is a PP pin and shows the rounded,
melted-looking appearance of the surface. (c) is a PMMA pin and shows the
roughened surface obtained with no build up on the trailing edge. All the
pins in Figure 17 were of diameter 6 mm.

Microscopic examination confirmed that very severe deformation of PC had
taken place with clear evidence of considerable strain in the frictional
direction (Figure 18(a)). PMMA (Figure 18(b)) presented a rather 'powdery'
appearance with many particles of material on the surface. The wearing away
of the PMMA pins proceeded in a more brittle manner with small particles chipped
out of the surface and with no accumulation of sheared or melted layers on the
trailing edge of the pin. The surface of PP on the other hand was relatively
featureless; as might be expected from a melted and refrozen layer.

Although there is clear evidence that PC had deformed by the shearing off
of layers, there was no evidence of catastrophic failure having taken place:
the shearing could be followed by the naked eye and took place over a time-
scale of ca. 1 s for a 6 mm pin. Nonetheless, temperatures well above the
commerical softening temperature were recorded with PC, and, when allowance
is made for the fact that these were averages over the whole surface, it does
seem possible that, under conditions of extreme (and probably locally rapid)
deformation, very high temperatures could be achieved by polymers such as PC.
These temperatures would be well above the limits set by the old ideas of the
temperature rise achieved in friction being limited by the melting point of
the lower melting point material which was based on the frictional properties
of metals. Any increase in melting point of the polymers due to the force
applied by the counterweight would be negligible since the maximum weight
used with the 6 mm pins was 2 kg and with the 1.5 mm pins was 500 g giving a
maximum stress of 3 MPa, which corresponds to ca. 30 bar. This would have an
insignificant effect on the melting point, variations of ca. 200 bar being
needed to cause an appreciable (ca. 10^0 K) change (Zoller 1978). It does
therefore appear that high temperatures can be reached during the deformation
of polymers, and, in the design of any system containing a polymer, consideration
must be given to the possibility of high temperature regions during deformation.

2.7 Conclusions and Discussion

A combination of high-speed photographic, pressure measuring and
thermal analysis techniques have been used to study the behaviour and inter-
action of explosives and polymers. Chemical interactions, for the materials
tested, were found to be of minor importance compared with mechanical consid-
erations in impact sensitisation. Pure explosives were found to ignite only
after rapid and severe deformation of the sample had occurred. In the
presence of sensitising grits however, this severe deformation was not
necessary for ignition. Both the fracture and thermal properties of an
additive are important in determining its sensitivity effect. A polymer
having a combination of high strength with low specific heat and low heat
of fusion, which tend to promote catastrophic failure, will be likely to

cause sensitisation. In order to test this hypothesis, two polymers were chosen on the basis of their strength and thermal capacity; polyester which has high strength and low capacity and high density polythene (HDPE) which has a low strength and high capacity. They were mixed with PETN and tested in the drop-weight machine in the same manner as the samples described earlier. The results obtained, together with a few comparison results from Table 5 are set out in Table 8. Thermal properties can be found in Table 6.

Table 8: 50% Heights for Explosive/Polymer Samples

Sample	50% height (cm)
PETN (pure	21.8 ± 1.0
PETN + HDPE	24.8 ± 1.5
PETN + PP	18.8 ± 0.8
PETN + Polyester	15.5 ± 1.0
PETN + PS	11.1 ± 0.3

These results confirm the predictions that polyester should sensitise and HDPE should not. In fact it appears that HDPE is acting as a desensitiser.

The conclusion reached, therefore, is that polymers which are most likely to sensitise are those such as PC which are tough below their glass transition temperature (as opposed to PMMA which behaves in a much more brittle manner), and are likely to fail catastrophically. Those least likely to sensitise are those which have a low glass transition temperature (PP or HDPE) and which deform in bulk with little local concentration of energy. Polyester is somewhat intermediate in behaviour (and sensitising effect) between PC and PMMA as it it tougher than PMMA but much more brittle than PC, and so fits quite well into the expected pattern.

In the case of the former the melting point of the particle is the important property (Bowden and Gurton 1949). That this is so is essentially because they are materials with well-defined melting points and relatively large latent heats: the hot spot is generated to the melting point. In contrast the polymeric materials which sensitise, soften over a range of temperatures and have low latent heats and thermal conductivities. If heat is produced by localised catastrophic failure hot spots will form. However, when softening of the polymer starts the material will still maintain a high viscosity. Continuing deformation will be able to contribute further temperature rises by viscous heating. Ther thermal losses in the case of a polymer are very low compared with most other materials because of the low latent heat, thermal capacity and conductivity, and the hot spot is not quenched so readily.

The friction experiment gave evidence of temperatures well above the softening point. In this experiment, an average temperature for a contact area of ca. 25 mm^2 was maintained. Local hot spot temperature would be

expected to exceed the values recorded. In other experiments in the laboratory, the temperature rise at the tip of a crack propagating in a polymer was recorded, again using I R techniques (Fuller, Fox and Field 1975). Two important results emerged from this work. The first was that temperatures well above the softening points were observed. Secondly, that the fracture surface energy increased with crack velocity. This latter result was explained by the high temperatures causing softening of the material at the crack tip thus requiring more energy to be expended in crack growth.

It is clear from the earlier work and the present work with explosive/polymer samples that some polymers can reach very high local temperatures during their deformation. This is clearly relevant to the safe handling of explosives since polymeric materials may be used for packaging or as binding materials in explosive composites. The results also have interest to studies of the fracture, friction, erosion and wear of polymers.

ACKNOWLEDGEMENTS

REFERENCES

Afanas'ev G.T. and Bobolev,V.K., 1961, Dolk. Akad. Nauk. SSSR 138,886.

Afanas'ev G.T., Bobolev, V.K. Kazazova,Yu Å and Karabanov,Yu F., 1972, Fiz. Gorenia i Vzryva 8(2) 229.

Afanas'ev G.T. and Bobolev V.K., 1971, Israel Program for Scientific Translations "Initiation of solid explosives by impact"

Andreev, K.K., Maurina, N.D. and Rusakova, Yu. A., 1955, Dokl. Akad. Nauk. SSSR, 105, 533.

Bean, C.M., 1973, Private Communication, AWRE.

Bolkhovitinov, L.G., Dokl. Akad. Nauk. SSSR, 125, 570.

Bolkhovitinov, L.G. and Pokhil, P.F., 1958, Aokl. Akad. Nauk. SSSR, 123, 637.

Bowden, F.P., Proc. Roy. Soc. 1950, 204

Bowden, F.P., 1963, 9th Int. Symp. Academic Press, N. York.

Bowden, F.P. and Yoffe, A.D., 1949, 3rd Symp. on Combustion and Flame Phenomena, p. 551, Baltimore: Williams and Wilkins Co.

Bowers, R.C., Romans,J.B. and Zisman, V.A., 1973, I. and EC Report, 12,2.

Bowden, F.P. and Gurton, O.A., 1949, Proc. Roy. Soc A 198, 337.

Bowden, F.P., Mulcahy, M.F.R., Vines, R.G. and Yoffe, A.D., 1947, Proc. Roy. Soc. A188, 291.

Bowden, F.P. and Thomas, P.H., 1954, Proc. Roy. Soc. A223, 29.

Bowden, F.P. and Yoffe, A.D., 1952, CUP, "Initiation and growth of explosion in liquids and solids".

Bowden, F.P. and Yoffe, A.D., 1958, Butterworths,"Fast reaction in solids".

Chaudhri, M.M. and Field, J.E., 1974, Proc. Roy. Soc. A340, 113.

Cundall, R.B., Palmer, T.F. and Wood, C.E., 1978, J. Chem. Soc. Faraday Trans., 1 74(6), 1339.

Dixon, W.J. and Massey F.J., 1957, McGraw-Hill "Introduction to statistical analysis".

Eirich, F.R. and Tabor, D., 1947, Proc. Camb. Phil. Soc. 44, 566.

Fox, P.G., 1970, J. Solid State Chem. 2, 491.

Freeman, E.S. and Carroll, B., 1958, J. Phys. Chem. 62, 394.

Fuller, K.N.G., Fox P.G. and Field, J.E., 1975, Proc. Roy. Soc. A341,537.

Gurrieri, S., Siracusa, G. and Cali, R., 1974, J. Thermal Analysis 6, 293.

Hauser, H.M. and Field, J.E., 1978, Thermochimica Acta 27, 1.

Heavens, S.N., 1973, University of Cambridge, Ph.D. Thesis.

Heavens, S.N. and Field, J.E., 1974, Proc. Roy. Soc. A338, 77.

Kholevo, N.A., 1946, Tr. Kazansk Khim. Tech. Inst. 10, 91.

Land, T., 1944, J. Iron and Steel Inst. 149, 481.

Maycock, J.N. and Vernecker, V.R. Pai, 1970, Thermochimica Acta 1, 191.

Ng. W.L., Field, J.E. and Hauser, H.M., 1976, J. Chem. Soc. Perkin. Trans. II, 637.

Parker, R.C. and Marshall, P.R., 1948, Proc. Inst. Mech. Engrs. 158, 209.

Ranby, B.G. and Rabek, J.F., 1975, Wiley, "Photodegradation, Photo-oxidation and Photodestabilisation of Polymers"

Reich, L., 1973, Thermochimica Acta. 5, 433.

Rideal, E.K. and Robertson, A.J.B., 1948, Proc. Roy. Soc. A195, 135

Robertson, A.J.B., 1948, J. Soc. Chem. Ind. 67, 221.

Rogers, R.N. and Morris, E.D., 1966, Analyt. Chem. 38, 412.

Taylor, W. and Weale, A., 1932, Proc. Roy. Soc. A. 138, 92.

Ubbelohde, A.R., 1948, Phil. Trans. A241, 199.

Walker, F.E. and Green Le Roy, 1976, US Government Report, AD-AO22812

Winter, R.E. and Field, J.E., 1975, Proc. Roy. Soc. A343, 399.

Zoller, P., 1979, J. Appl. Polymer Sci. 23, 1051.

FIGURE CAPTIONS

1. Activation energy plot for the thermal decomposition of PETN for various values of reaction order n. The n value which gives the best straight line segments is one appropriate to the reaction (here 0.8). These two steps (see dashed line) corresponding to sublimation, stage I, and decomposition stage II.

2. Experimental arrangement at instant of impact, W; drop-weight; G, glass blocks; M, mirrors; S, sample. The upper glass block is attached to the weight.

3. Impact on a disc of PP. The sample deforms by bulk plastic flow throughout. Diameter of field of view 20 mm. Frame time/µs : a,0; b,70;c,266. The zero times given in this and subsequent sequences do not correspond to time after initial contact.

4. Impact of a disc of PS. The sample deforms initially by bulk plastic flow (frames a and b) but then deforms catastrophically (frame c). Diameter of field of view, 2.5 mm. Frame times/µs : a,0;b,21;c,28.

5. Diameter versus time traces for impacts on PP and PS. Note that the diameter of the PS has approximately doubled before the catastropic failure, but that the PP disc has a final diameter several times its initial value.

6. Micrographs of a deformed PS disc showing that the catastrophic failure is a result of fracture and localised shear. The enlarged view in (b) is from region S in (a). The view has been rotated so that the shear bands are horizontal.

7. Impact on a pellet of PETN. Frame a shows the 5 mm diameter pellet before impact. Rapid flow and jetting occur as for powdered layers. Fusion of the layer starts in frame d. The whole layer is transparent and flowing rapidly by frame g when the first to two ignition sites forms. The circular feature in frame h is an artifact. Diameter of field of view 20 mm. Frame times/µs : a,0;b,67;c,221;d,308;e,389; f,469;g,476;h,482;i489.

8. PETN pellet surrounded by 5 PS discs See text for details. Two ignition sites at the polymer/explosive interface are labelled in frames d and e. Diameter of field of view 20 mm. Frame times/µs :a,0; b,91;c140;c,161;e,168;f,175.

9. 25 mg disc of PETN containing a PS disc. Three ignition sites are labelled. Field of vuew 20 mm. Frame times/µs: a,0;b,14.

10. A PP disc (light) pressed into an HMX pellet. The first frame is before impact. Considerably bulk deformation of the PP occurs but there is no ignition of the explosive. Field of view 20 mm. Frame times/µs: a,0;b,91;c,161;d,214;e,247;f,402.

11. Similar to figure 10 but with a PC disc: except that impact has already occurred in frame a. The PC fails catastrophically. The first of several ignition sites can be detected in frame d. Field of view 20 mm. Frame time/µs;a,0;b,34;c,94;d,121;e,135;f,147.

12. Experimental arrangement for obtaining pressure-time curves. W, drop-
weight; H, R1,R2,R3, hard steel rollers; C, cylindrical guiding sleeve;
S, sample.

13. Stress-strain curves for samples of (a) PP, (b) PC. Catastrophic
failure of the PC sample occurs at a strain of ca. 1.8. No discontin-
uities are observed in the PP curve.

14. Experimental arrangement for friction experiments. D, detector;
S, slits; CD, chopper disc; SD, sapphire disc; PP polymer pin;
BA, balance arm; W, counterweight; DS, drive shaft.

15. Calibration curves for the friction apparatus (a) high temperature
region (b) low temperature region.

16. Examples of the traces obtained with the apparatus (a) is a soldering
iron at 575 K (b) a small diameter PC pin and (c) a large diameter
PC pin. H is the signal strength when there is no filter between
source and detector and H' the strength when a PMMA filter is inter-
posed between source and detector.

17. Polymer pins after friction experiments. (a) a PC pin showing many
layers which have been sheared off and built up on the trailing edge
(b) a PP pin which has rounded and shows evidence of melting (c) a
PMMA pin which has a roughened surface caused by small particles
being brittly chipped out of the surface.

18. Micrographs of polymer pin surfaces after friction experiments.
(a) PC and shows considerably strain in the frictional direction.
(b) PMMA which has a powdery appearance with many small particles
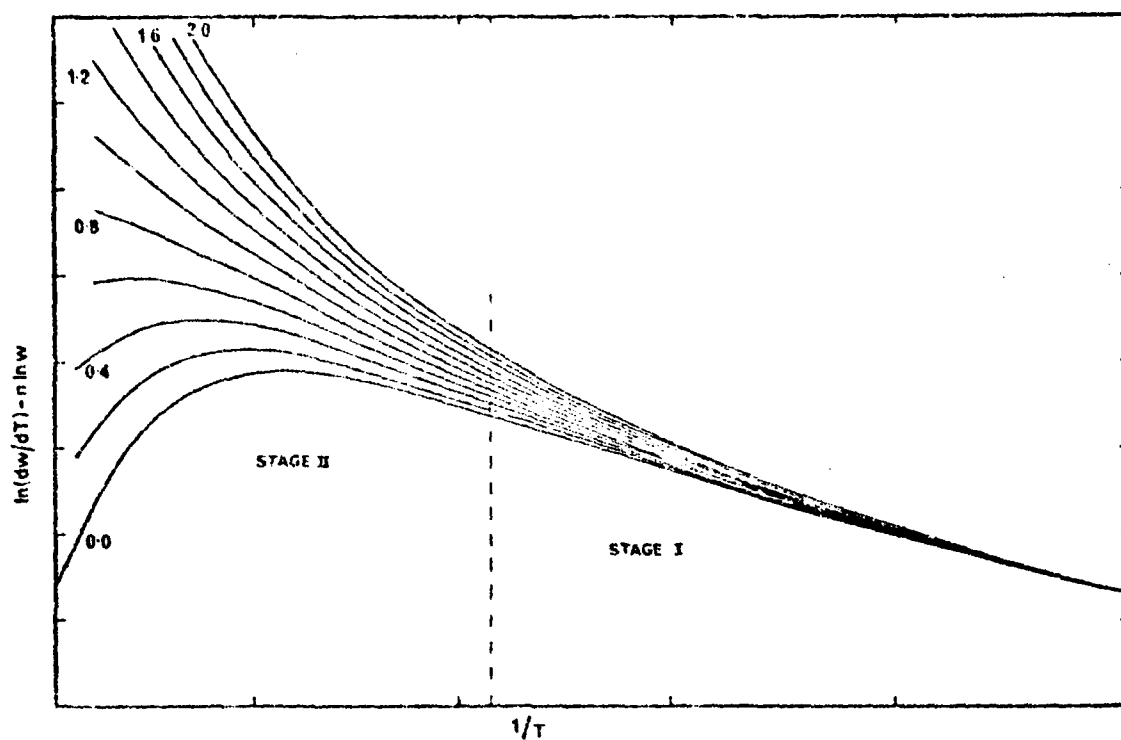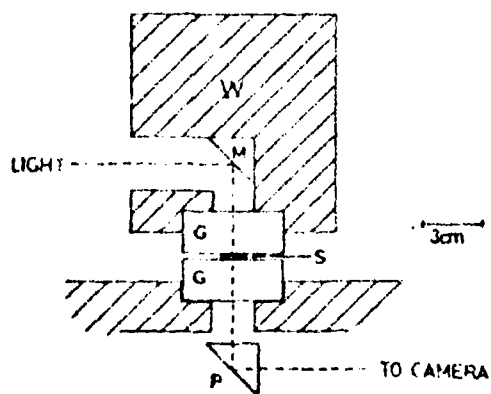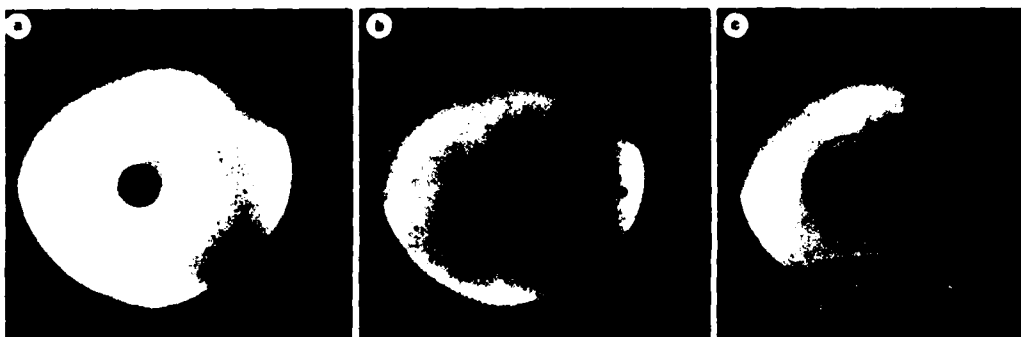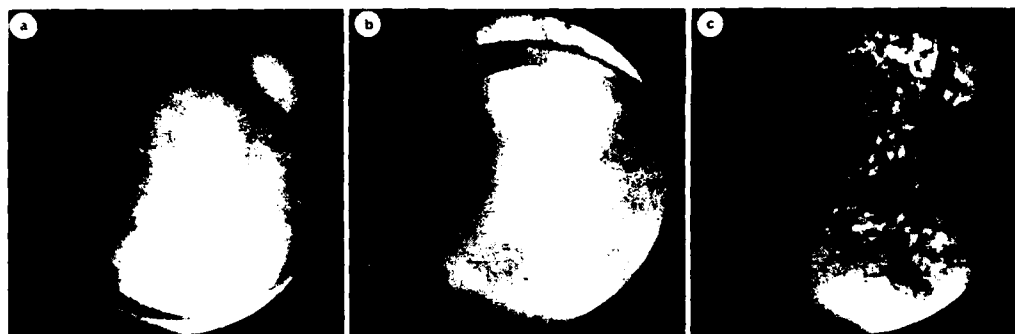chipped out of the surface.

FIG 1

FIG 2

FIG 3

FIG 4
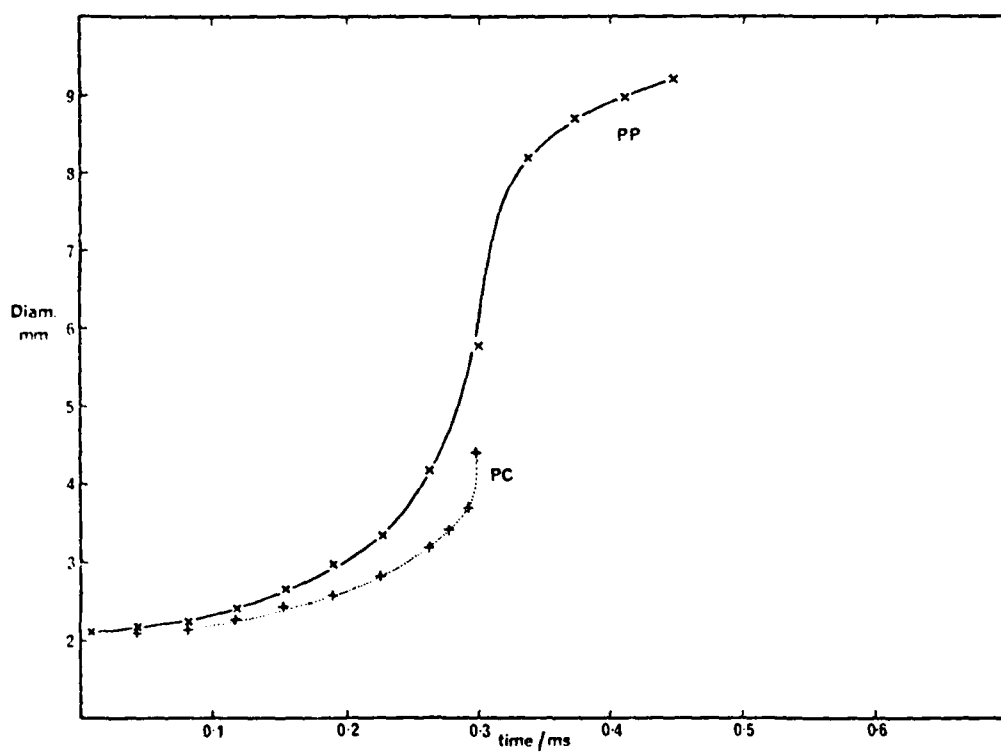
FIG 5
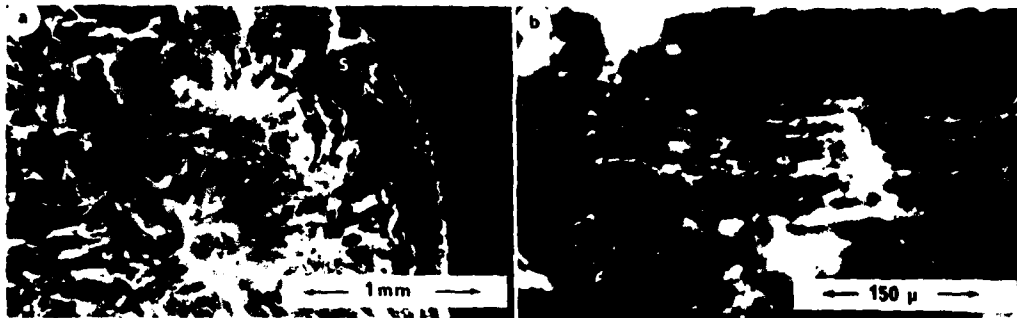
FIG 6
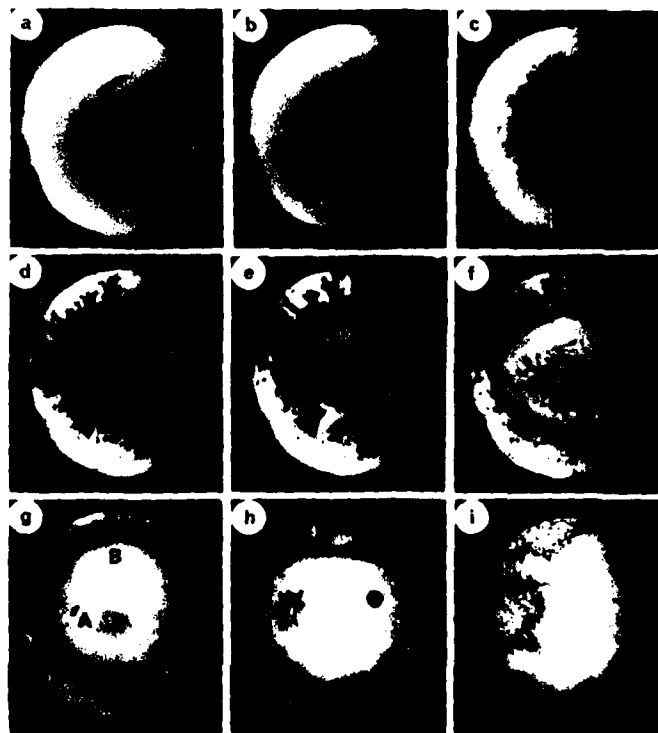
FIG 7

FIG 8

FIG 9
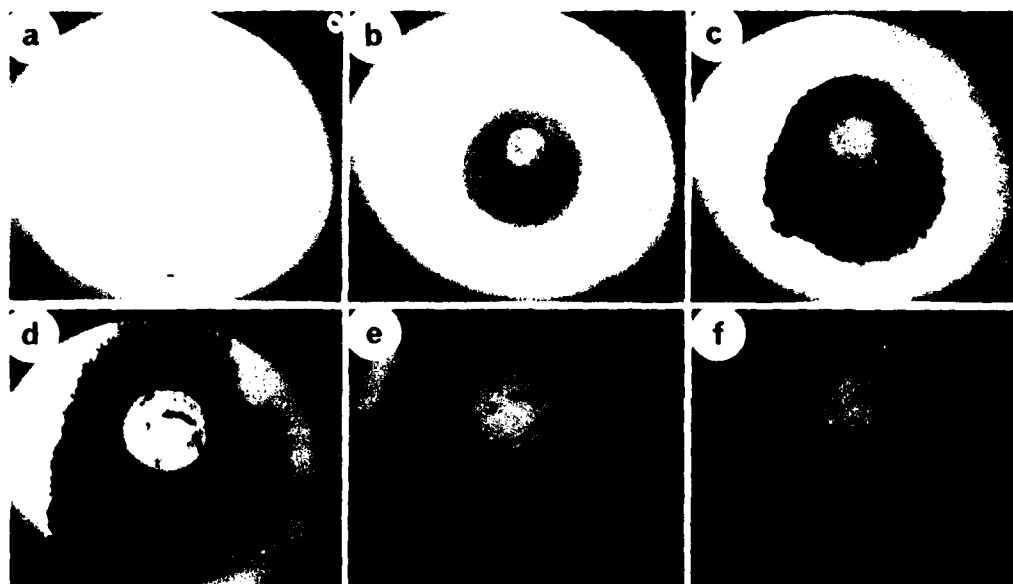
FIG 10
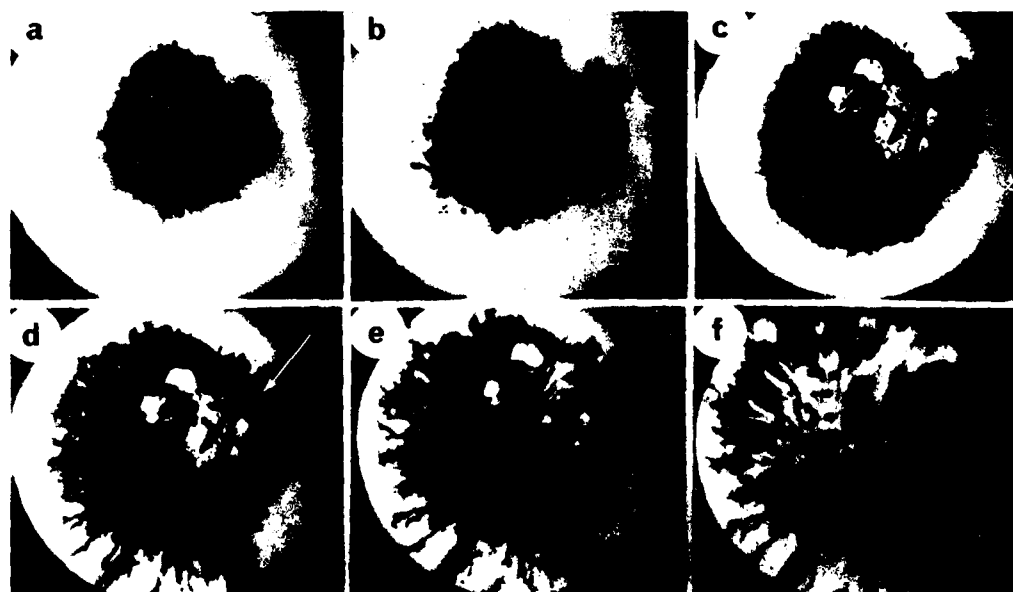
FIG 11
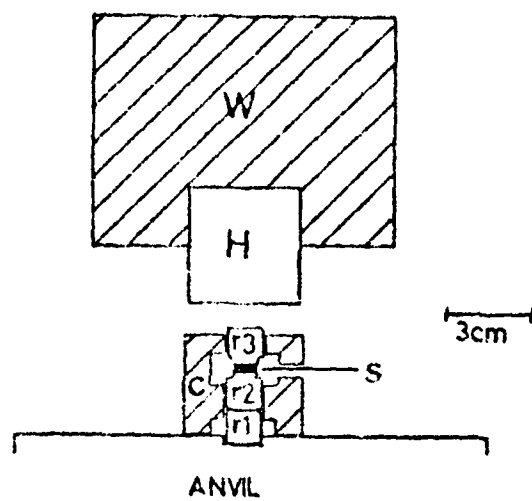
FIG 12
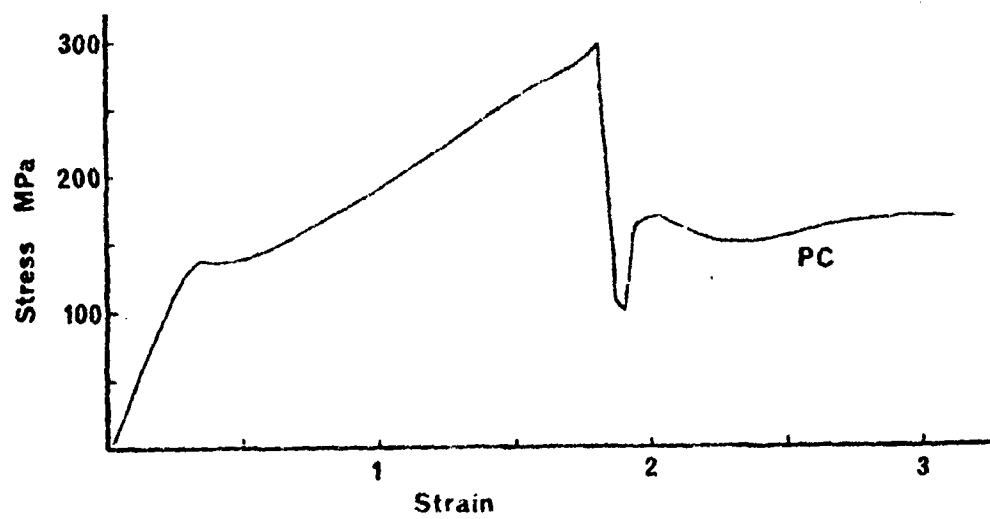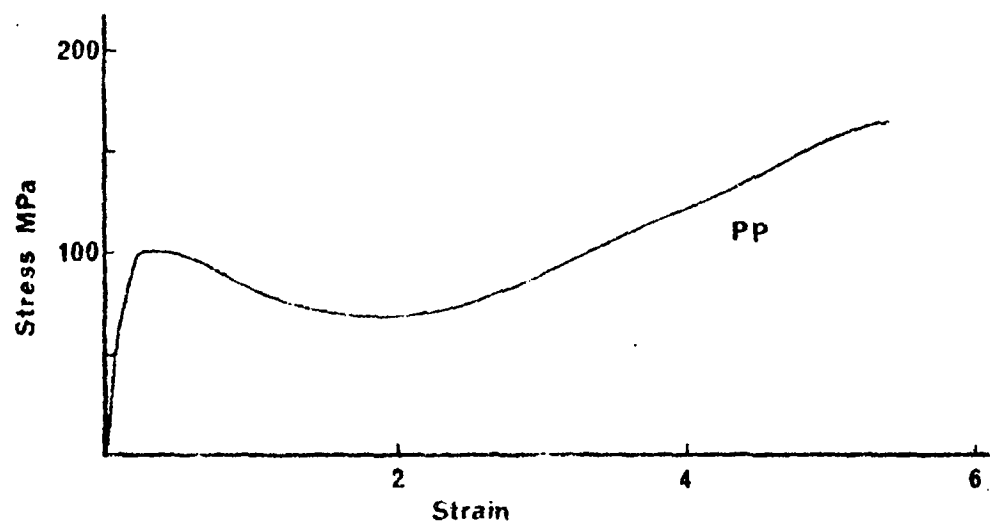
FIG 13
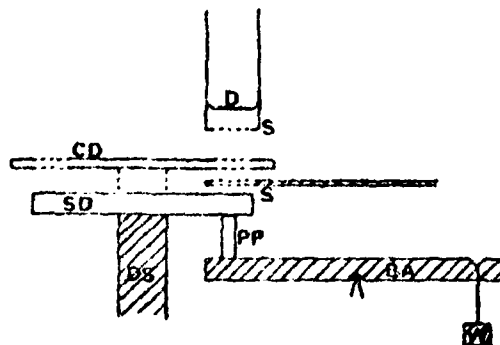
FIG 14
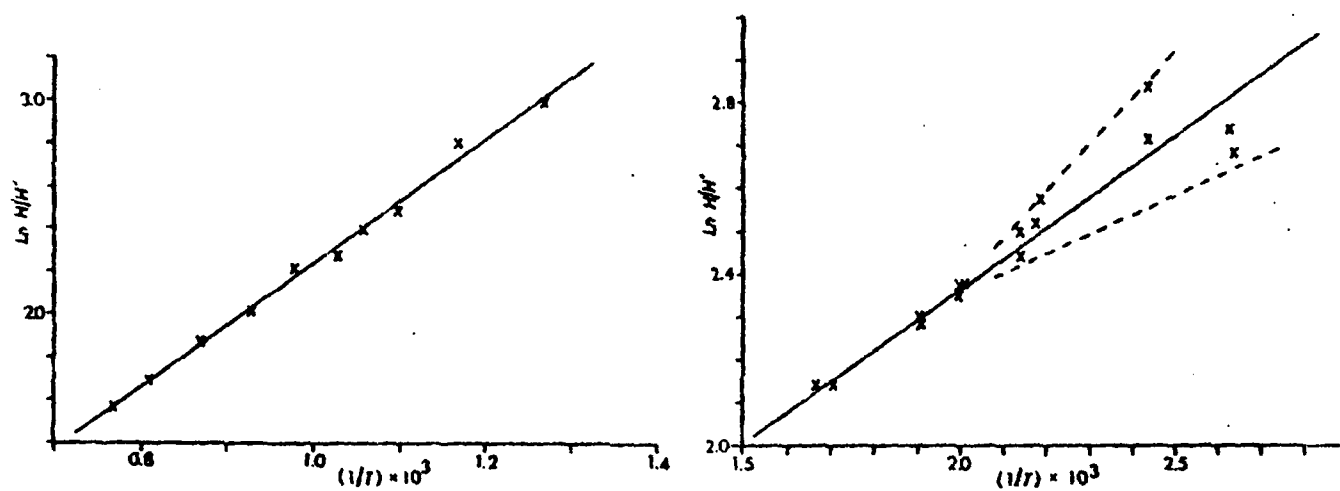
FIG 15
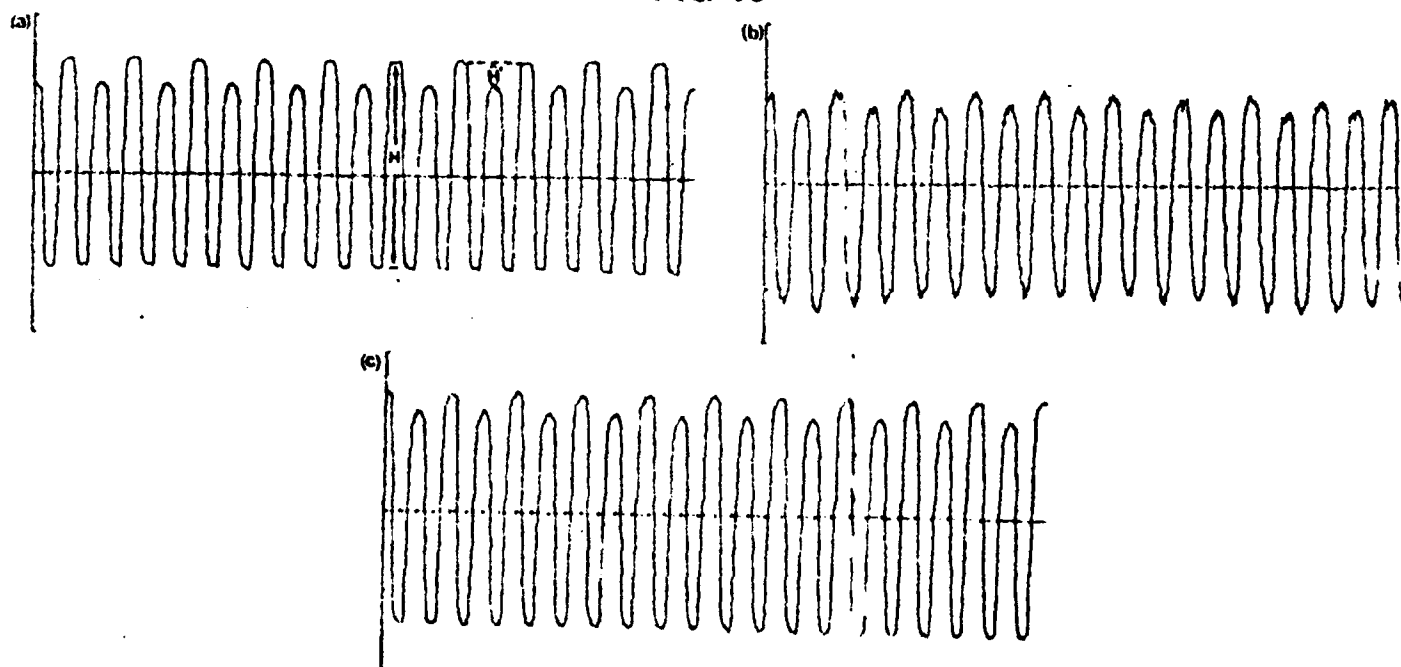
FIG 16
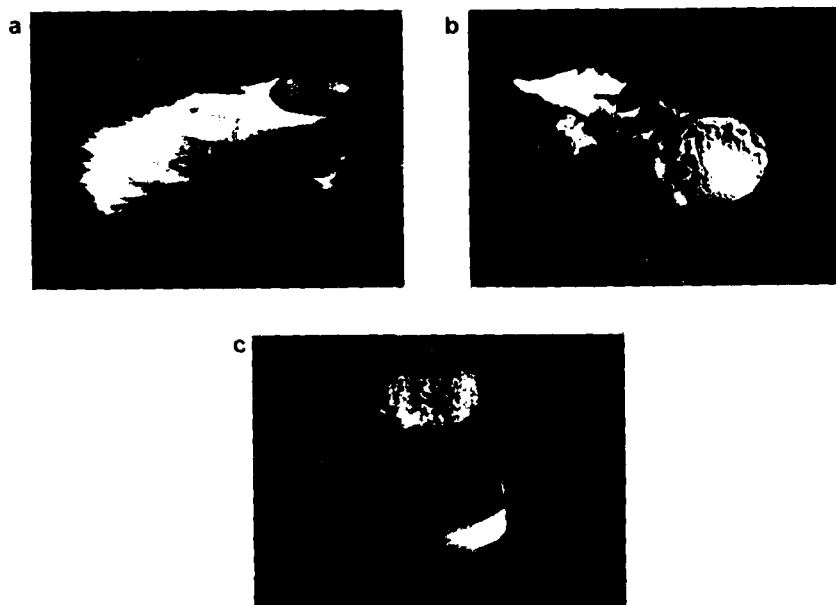
FIG 17
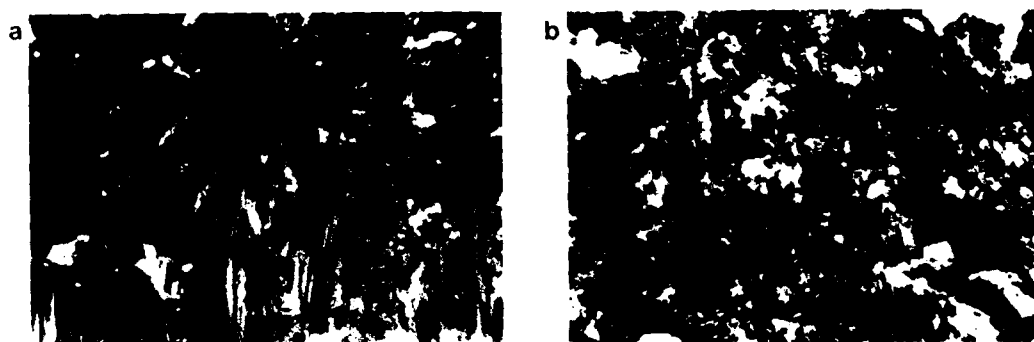
—— 1mm ——

FIG 18

The remaining three sections of this report (3,4,5) are on reaction kinetics and their analysis. All have been published in the open literature.

For completeness, reference is given to a paper (Chaudhri et al, 1977) based on work performed by Dr. Chaudhri when he visited Picatinny, and to other papers published by the gr , :nce 1977.
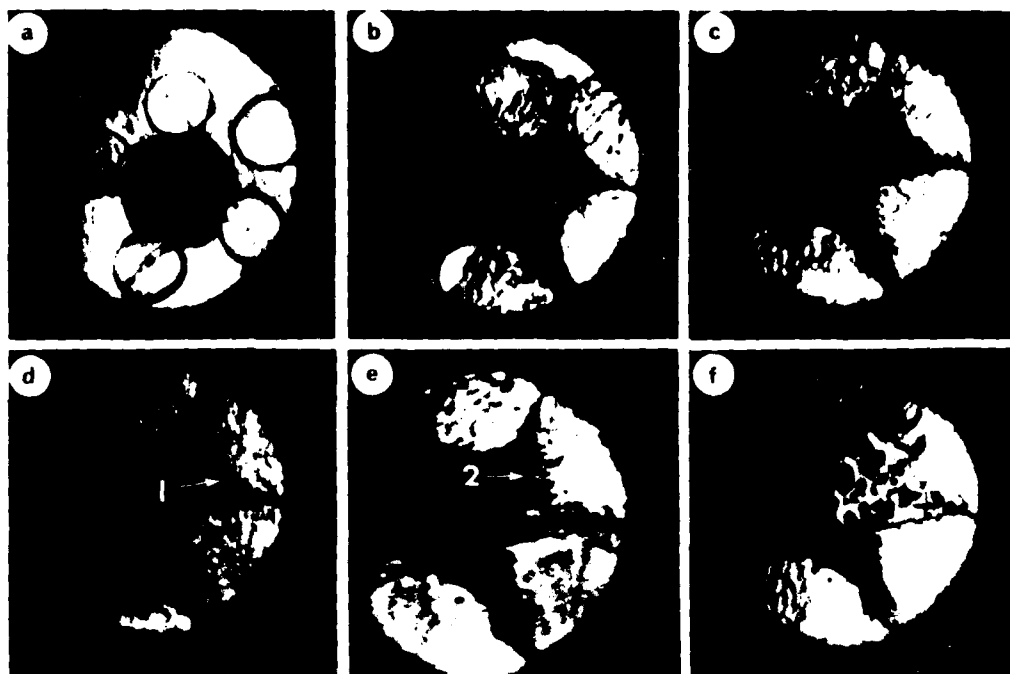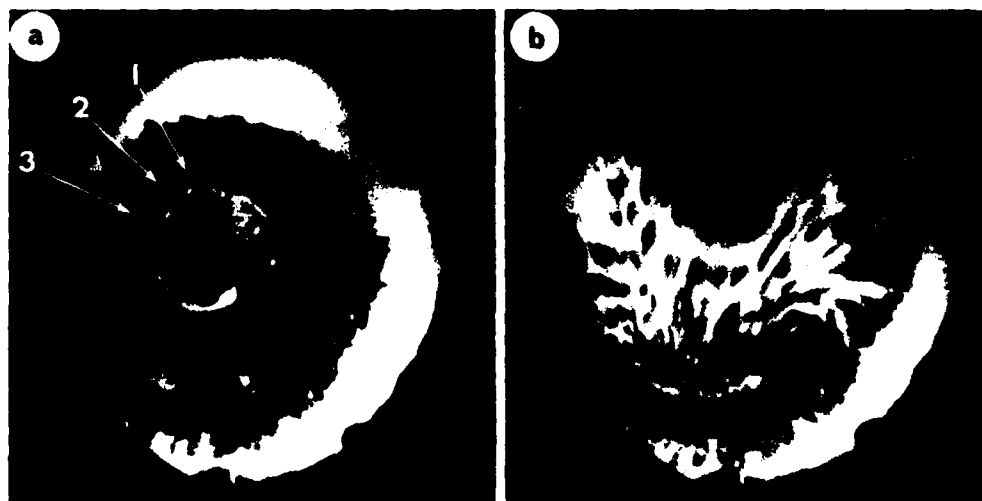
M.M. Chaudhri and J.E. Field, "Fast Decomposition in the Inorganic Azides", from Energetic Materials, Vol. 1, Ed. H.D. Fair and R.F. Walker (Plenum, 1977).

J.T. Hagan and M.M. Chaudhri, "Fracture Surface Energy of High Explosives PETN and RDX", J. Mater. Sci. 12 (1977) Letters 1055-58.

M.M. Chaudhri, W.L. Garrett, O. Sandus and N. Slagg, "The High Velocity Detonation of Single Crystals of Alpha-Lead Azide", Propellants and Explosives, 2, 91-93 (1977).

R. Patel and M.M. Chaudhri, "Differential Scanning Calorimetric Studies of Decomposition of Beta-Lead Azide", Thermo. Chimica. Acta. 25, 247-251, (1978).

T.B. Tang and M.M. Chaudhri, "Dielectric Breakdown of Ionic Azides", Conf. on Elect. Insulation and Dielectric Breakdown, Washington, (1979).

T.B. Tang and M.M. Chaudhri, "Dielectric Breakdown by Electrically Induced Decomposition", Nature 282, 5734, 54-55 (1979).

T.B. Tang and M.M. Chaudhri, "The Thermal Decomposition of Silver Azide", Proc. Roy. Soc. A369, 83-104, (1979).

T.B. Tang, "Analysis of Isothermal Kinetic Data from Multi-Stage Decomposition of Solids", Thermochimica Acta, 41, 133-136 (1980).

SECTION 3

NEW METHOD FOR TG AND DSC DATA ANALYSIS

H. M. HAUSER AND J. E. FIELD

Physics and Chemistry of Solids, Cavendish Laboratory, Madingley Road, Cambridge (Gt. Britain)

(Received 28 November 1977)

ABSTRACT

The paper describes a graphical computer method for analysing TG and DSC traces which gives all three reaction parameters (E, A, and n) characterising an nth-order reaction from a single trace. If the reaction proceeds in multiple stages (E, A and n) triplets can be obtained for each stage. The computer programmes are basically simple and use little computing time (typically a few seconds). The advantages of the approach over earlier methods are discussed. As a test of the method, results on the dehydration of calcium oxalate monohydrate are described.

INTRODUCTION

The deduction of the reaction parameters E (activation energy), A (frequency factor), and n (reaction order) from TG, and DSC traces is clearly of interest. A number of methods have been used in the past to do this but all have unsatisfactory features. In the work described here a number of Fortran programmes were written to extract all three reaction parameters of an nth-order reaction from a single TG, or DSC trace. The programmes were run on the Cambridge IBM 370 165 computer, and the plotter was used for graphical output. So that the advantages of the present approach can be appreciated earlier methods are briefly discussed.

EARLIER METHODS

Murray and White[1] have shown that the temperature at the reaction peak of DTA traces can be used to obtain E and A from a number of traces if a first order reaction (eqn. 1) is assumed, where w is the fractional residual weight, t the time, T the temperature and R the gas constant.

$$\frac{dw}{dt} = - A \exp \left(- \frac{E}{RT} \right) w \tag{1}$$

If eqn. (1) is differentiated to obtain the maximum for dw/dt then eqn. (2) can be derived, where $\phi = dT/dt$ is the heating rate and T_m the temperature at the rate maximum.

$$\ln \left(\frac{\phi}{T_m^2} \right) = \ln \frac{AR}{E} - \frac{E}{R} \cdot \frac{1}{T_m} \tag{2}$$

A plot of $1/T_m$ versus $\ln (\phi/T_m^2)$ yields E/R as the slope and $\ln (AR/E)$ as the intercept of the straight line with the ordinate. The main disadvantage of this method is that it only uses a single point (T_m) from a trace to produce one point on the activation energy plot. A number of experiments are needed to obtain a reliable value for E. There is also the limitation that the theory only works for a first-order reaction.

Kissinger[2] showed that the technique can be extended to an nth-order reaction by deriving eqn. (3).

$$\frac{E}{RT_m^2} = A\, n\, w_m^{n-1} \exp\left(-\frac{E}{RT_m}\right) \tag{3}$$

He shows in his paper that the product $n\, w_m^{n-1}$ is independent of the heating rate (ϕ) and almost equal to unity. Therefore, eqn. (3) effectively reduces to eqn. (2). The approach again makes poor use of the information contained in a DTA trace.

Ozawa's analysis[3] of TG traces begins with a general form of reaction equation.

$$\frac{dw}{dt} = -A \exp\left(-\frac{E}{RT}\right) f(w) \tag{4}$$

This is integrated by Ozawa who shows that the solution to the right-hand side of the equation is a polynomial in the variable E/RT. Equation (5) is an approximate formula which relates the heating rate ϕ with E.

$$\log\phi_1 + 0.4567\,\frac{E}{RT_1} = \log\phi_2 + 0.4567\,\frac{E}{RT_2} \tag{5}$$

where T_1 and T_2 correspond to the same fractional decomposition (w) of the sample. Since a plot of $\log\phi$ versus $1/T$ can be obtained for each value of w, Ozawa aggregates all these results in a master-curve with a gain in accuracy of the final result. Equation (5) only assumes that the function $f(w)$ is constant for a given value of w.

This method also needs a number of experiments at different heating rates to generate enough data for a single activation energy plot. Although the method was developed for thermogravimetric data, it can be applied to DSC data by integrating the peaks to give values of w. A theoretical analysis of such a process is given by Reed et al.[4].

Borchardt and Daniels[5] describe a method which allows E, A and n to be determined from the shape of a DTA curve. Their approach was applied to reactions in the liquid phase. The type of reaction to which this method is applicable must have a single rate constant and the activation energy must not vary with temperature. By considering the heat transfer equation of the calorimeter eqn. (6) was obtained

$$-\frac{dN}{dt} = \frac{N_0}{KA'}\left\{C_p\,\frac{d\Delta T}{dt} + K\Delta T\right\} \tag{6}$$

where N is the number of moles present, N_0 the initial number, K the heat transfer coefficient, A' the area under the DTA curve, C_p the heat capacities of the two liquids and ΔT the temperature difference between the two cells. Integration of eqn. (6) with respect to time gives

$$N = N_0 - \frac{N_0}{KA'}\left\{C_p\,\Delta T + Ka\right\} \tag{7}$$

where a is the area under the DTA curve up to the present temperature.

The expression for the rate constant k of a reaction of order n is

$$k = -V^{(n-1)}\frac{dN/dt}{N^n} \tag{8}$$

where V is the volume. Substituting eqns. (6) and (7) for dN/dt and N gives

$$k = \left\{\frac{KA'V}{N_0}\right\}^{n-1} \frac{C_p\,\dfrac{d\Delta T}{dt} + K\Delta T}{\left\{K(A' - a) - C_p\Delta T\right\}^n} \tag{9}$$

In order to obtain reaction parameters, Borchardt and Daniels[5] assumed a value for n. This allowed k to be calculated. A plot of ln k versus $1/T$ (activation energy plot) yields a straight line if, and only if, the correct value of n has been assumed, thus values of E, A and n can be obtained. The main difficulty of this method is the number of plots that have to be made for each value of n until the points lie on a straight line.

A number of computer programmes are presented by Benin et al.[6] and used to solve three problems, namely (i) the production of thermograms given the reaction parameters E, A, n and given that the reaction is of the nth-order type; (ii) the calculation of the (E, A, n) triplet from an experimental thermogram — this is the inverse to problem (i); and (iii) the determination of the reaction parameters and the complex reaction mechanism from a given experimental thermogram. The first problem is a straightforward function plot of the solution to the nth-order reaction equation. The second problem is more difficult, and presents itself to anyone who wants to obtain reaction parameters from experimental data. Benin et al.[6] treat it as a problem in curve fitting. They minimise the discrepancy between the experimental data and the calculated function by taking as the discrepancy criterion the maximum deviation of the function from the data. The solution of the third problem is an attempt to reveal the mechanism of a chemical reaction. The programmes become quite involved as they work out activation energies for each section of the thermogram by using a plot of reaction rate versus $1/T$ for a constant amount of conversion, α, but different heating rates.

The most general form of the fit function assumes a decomposition process which proceeds in a number of individual stages. Each stage consists of an elementary nth-order reaction, i.e., eqn. (1) with A, E and w replaced by A_i, E_i and w_i, respectively, where "i" denotes the variable belonging to the ith stage of the reaction. The programme which optimises the fit of this function to the data takes up to 4 h of computing time. This makes the method rather expensive. Another weak point is the discrepancy criteria between the data and the fit, which is taken as the maximum difference. It is well known that the data points towards the end of a decomposition process become less reliable due to impurities and zero errors. But these points have the same weight in the analysis as all the others.

Schempf et al.[7] describe a programme which fits a least square polynomial to the weight-loss curve. The quantity dw/dt is calculated by differentiation of the polynomial. A straight line is then fitted to a plot of log k versus $1/T$, and the least square criterion is used again. The reaction order is assumed to be one, and no attempt is made to eliminate the deviations from an ideal reaction at the beginning and end of the weight-loss curve. Our work shows that this is very critical and can be obtained from an Arrhenius plot performed by the computer.

NEW METHOD

The method developed was based on the ideas of Borchardt and Daniels[5]. Our data were obtained from both a thermobalance (Stanton Redcroft) and a differential thermal calorimeter (Perkin-Elmer DSC-2).

The analysis assumes a reaction which can be described by

$$\frac{dw}{dt} = - A_i \exp\left(- \frac{E_i}{RT}\right) f_i(w) \tag{10}$$

Since the heating rate h (deg min^{-1}) is constant, the time variable can be eliminated from eqn. (10) by putting $dT/dt = h/60$ (deg sec^{-1}).

Taking natural logarithms on both sides gives

$$\ln\left(-\frac{dw_i}{dt}\right) - \ln f_i(w) = \ln\frac{A_i \times 60}{h} - \frac{E_i}{RT} \tag{11}$$

Note that $(-dw/dt)$ is a positive quantity since the fractional residual weight decreases with increasing temperature.

A plot of $\{\ln(-dw_i/dt) - \ln f_i(w)\}$ versus $\{1/T\}$ only yields a straight line if $f_i(w)$ has been chosen correctly. In the case of $f_i(w) = w^n$ the reaction order n is varied until a straight line is found. The activation energy E can be obtained from the slope of this plot, the frequency factor A from the intercept on the ordinate and the reaction order n is determined by the straight line criterion.

This analysis can also be applied to the DSC data since the basic eqn. (12) only differs from (10) by constants.

$$\frac{dQ}{dt} = \pm \Delta H(w_o - w_t) A \exp\left(-\frac{E}{RT}\right) f(w) \tag{12}$$

The $+$ $(-)$ in the equation corresponds to an exothermic (endothermic) reaction where, Q is the heat given off by the sample, ΔH is the enthalpy change of the entire reaction, w_0 is the initial weight and w_t is the rest weight, and the other parameters are as defined previously.

Taking logarithms gives

$$\ln\left(\frac{dQ}{dt}\right) - \ln f(w) = \ln \Delta H(w_o - w_t) A - \frac{E}{RT} \tag{13}$$

This time dQ/dt at temperature T is the measured quantity and w needs to be calculated. This is easily done since, if the reaction results in a weight loss

$$w_t = \frac{1}{\Delta H} \int_0^t \frac{dQ}{dt} dt \tag{14}$$

The computer numerically integrates dQ/dt to yield the weight at time t. A plot of $\{\ln dQ/dt - \ln f(w)\}$ versus $1/T$ produces E, A and n (if $f(w) = w^n$) in the same way as for the weight-loss curves above. The slope is again $-E/R$ and the intercept is $\ln \Delta H(w_0 - w_t).A$.

In practice the data from the TG or DSC is recorded on 8 track ASCI paper tape. This information is then read into disc files of the computer. These files can be used by the programmes which calculate the activation energy, etc. After these programmes have run, the plotter output is viewed on a television screen. Only if the plot is satisfactory is a copy obtained from the plotter for the final analysis. The dimensions correspond to the original output of the chart recorder so that a direct comparison is possible. Different pen colours are used to differentiate between the raw data (black) and the theoretical fit to the data (green). These colours are represented in Fig. 1 as a broken line (black) and a full line (green).
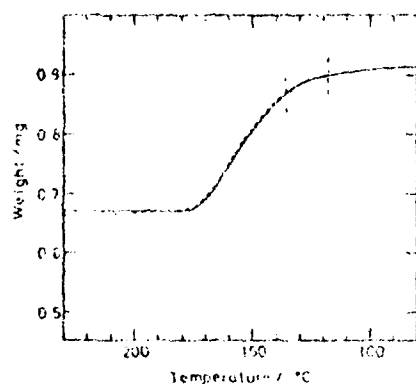
Fig. 1. Weight loss curve of Ca C₂O₄H₂O analysis. The dashed line is the original data and the full line the replot using the computed (E, A, n) triplet for the three straight line sections which are separated by vertical dashed lines.

The differential programme[*]

There are three different ways in which differentials to the weight-loss curve were obtained. The first uses differences and produces a noisy differential curve, which is, however, nearest to the original data. The other two use a polynomial fit, and a spline fit, respectively. The polynomial fit, usually of 25th order, is generally good but produces artificially large undulations over straight regions of the curve. The best results were obtained by a cubic spline fit. This programme fits a third order curve to sections of the data, and joins them in such a way that the function and the first two derivatives are continuous. The programme uses a standard subroutine from the Harwell Fortran library, which chooses its own knots (points where two splines meet) according to the behaviour of the original curve. This means that over a straight part of the curve a long section can be fitted by a single cubic spline, whereas at places of greater variation, smaller sections are chosen to be approximated. The differential of the curve is then obtained by differentiating the third order spline. The fit of the spline and the differential is very accurate. The amount of data smoothing achieved by this fit suits the purpose of the following programme (next section) best.

The programme to find E, A and n

It is assumed in this analysis that the reaction that leads to the weight-loss curve is at least piece-wise of the nth order, i.e. follows eqn. (10) with $f_i(w) = w^n$. This programme plots $\{\ln(-dw/dt) - n \ln w\}$ versus $1/T$ for different values of n. The values of dw/dt and of w are obtained from a file that was created by the previous programme and contains the smoothed weight-loss data and the differential in the form of the spline parameters. The value of n is taken as zero for the first plot and then increased by 0.2 ten times up to $n = 2$. These eleven lines have different curvatures. The straightest of them can easily be selected by eye and this n value is then taken as the reaction order. The slope yields E and the intercept A. The resulting triplet of numbers (E, A, n) are necessary and sufficient to characterise an nth-order reaction. The type of reaction, i.e. $f(w) = w^n$ can be changed easily so that the programme is applicable to reactions of any type, i.e. $f(w)$ can have any form (e.g. random chain scission).

---

[*] This and the following programmes can be obtained from the authors.

The programme to produce a theoretical fit from the (E, A, n) triplet

This programme allows the production of a weight-loss curve with up to four different sections each of which has its own E, A and n factor. It was implemented on a Hewlitt Packard Desk top calculator and plotter of the type HP 9825. The theoretical plots produced in such a way fit the original weight-loss curve very well. They also provide a useful check that all the calculations necessary to produce this triplet were correct, and produce a good fit.
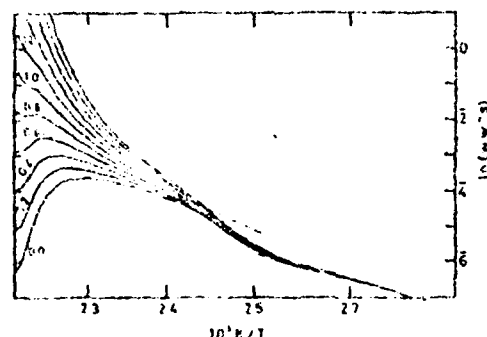
Fig. 2. Activation energy plot for various values of reaction order n. The n value which gives the best straight line segments is the one appropriate to the reaction there 0.6). There are three steps to the reaction but the first two correspond to only ca. 2% of the weight-loss.

TEST OF METHOD

The dehydration reaction of calcium oxalate monohydrate

$$Ca\ C_2O_4H_2O \rightarrow Ca\ C_2O_4 + H_2O$$
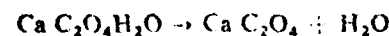
is well understood and values for the reaction parameters can be obtained from the literature[8, 9]. It therefore provides a good test case for the new analysis method. Figure 1 shows the weight-loss curve of a sample of $Ca\ C_2O_4H_2O$. The dashed curve represents the original data and the full curve the theoretical fit based on the computed (E, A, n) triplet. Figure 2 shows the activation energy plot. The number at the end each line gives the reaction order that is assumed for the calculation of the corresponding line. The straight lines which approximate the curves best are used to obtain (E, A, n) triplets for the three sections. Since these (E, A, n) triplets completely specify the reaction the original weight-loss curve can be modelled (full curve Fig. 1). The results obtained with this method, and literature values are summarized in Table 1. All our experiments were performed at a heating rate of 10 deg min^{-1}. The results obtained in this way have an error of $\pm$ 5 kJ mol^{-1} which is due to the variance of the samples themselves. The method itself has much greater accuracy. It was found that the best straight line could be fitted to a curve corresponding to a reaction order of 0.6

TABLE 1

E (kJ mole^{-1})	ln A	Ref.
87	19.8	This work
84	17.5	This work
88	21.0	8
92		9

which indicates a surface reaction (theoretically 2/3). It can also be seen on Fig. 2 that there are three distinct stages of the reaction. The first two, however, correspond to only 2% of the weight and are attributed to volatile substances on the surface. This shows the sensitivity of the method used especially considering that the vertical axis has a logarithmic scale. The real dehydration reaction is represented by the last straight line segment.

The method outlined in this paper has recently been successfully applied[10] to decomposition studies of P.E.T.N., P.E.T.N. with fillers, high density polyethylene (HDPE) and polytetrafluoroethylene (PTFE).

ACKNOWLEDGEMENTS

REFERENCES

1 P. Murray and J. White, *Trans. Br. Ceram. Soc.*, 54 (1955) 204.
2 H. E. Kissinger, *Anal. Chem.*, 29 (1957) 1702.
3 T. Ozawa, *Bull. Chem. Soc. Jpn.*, 38 (1965) 1881.
4 R. L. Reed, C. Weber and B. S. Gottfried, *Ind. Eng. Chem. Fundam.*, 4 (1965) 38.
5 H. J. Borchardt and F. Daniels, *J. Am. Chem. Soc.*, 79 (1957) 41.
6 A. I. Benin, I. S. Israilit, A. A. Kossoi and Yu. E. Mal'kov, *Fiz. Goreniya Vzryva*, 9 (1) (1973) 54.
7 J. M. Schempf, F. E. Freeberg, D. J. Royer and F. M. Angeloni, *Anal. Chem.*, 38 (3) (1966) 520.
8 S. Gurrieri, G. Siracusa and R. Cali, *J. Therm. Anal.*, 6 (1974) 293.
9 E. S. Freeman and B. Carroll, *J. Phys. Chem.*, 62 (1958) 394.
10 H. M. Hauser, *PhD Thesis*, University of Cambridge, 1977.

ANALYSIS OF ISOTHERMAL KINETIC DATA
FROM SOLID-STATE REACTIONS

TONG B. TANG and M. M. CHAUDHRI

Physics and Chemistry of Solids, Cavendish Laboratory, Madingley Road, Cambridge UK

In most solid state reactions the reaction velocity can be described as a product of two functions $K(T)$ and $f(1-\alpha)$ where T is the temperature and α the degree of conversion of the solid reactant. The physical interpretation of these functions is discussed, and a systematic method is described by which $f(1-\alpha)$ of a reaction is identified from its kinetic data. $K(T)$ and the reaction mechanism are then determined. This method has been successfully applied to analyse the kinetics of the thermal decomposition of silver azide.

In a solid-state reaction, the reaction velocity is given by $-d/dt\,(1-\alpha) = \dot{\alpha}$, where $\alpha = \alpha(t)$ is the fraction of the solid reactant which has reacted by time t. Its kinetics can be solved by determining $\dot{\alpha}$ as a function of temperature and the global amount of reactant left. This phenomenological knowledge is a necessary, though not sufficient, condition for elucidating the reaction mechanism. It is necessary to formulate the reaction velocity in terms of the global variable α, because there is a continuous collapse of structure in the reactant. Furthermore, the local concentration of the reactant varies throughout the reaction volume and cannot be used as a state variable. In fact, unlike the case of a homogeneous reaction in the liquid or gaseous phase, there is no real 'reaction order' with respect to any reactant in a reaction involving condensed matter whose mechanism is usually of the heterogeneous type.

If the reaction proceeds isothermally, it is observed empirically that (α, t) curves corresponding to different temperatures T are isomorphic to one another, at least within a range of T, i.e., by a linear scale change in t, different curves can be superimposed [1]. It follows that $\dot{\alpha}$ is a separable function:

$$(\dot{\alpha})_{\text{isothermal}} = K(T)f(1-\alpha). \tag{1}$$

Here $f(1-\alpha)$ may change in different ranges of T or α. For every $f(1-\alpha)$, there corresponds a single $K(T)$. It should be noted that experimental data may be adequately analysed by (1) only if it has been ensured that the temperature distribution in the sample is *sufficiently uniform and constant*. Furthermore, the theoretical significance of $K(T)$ and $f(1-\alpha)$ determined from the data should always be examined with regard to the class of mechanisms they indicate. A question of consistency arises in this respect. In the literature, coherent and integrated accounts of the physical (as contrasted with the formal) meanings of $K(T)$ and $f(1-\alpha)$ are not easily found. A discussion on their interpretations therefore forms the first part of this paper. In the second part we propose an efficient method of determining, with confidence, both $f(1-\alpha)$ and $K(T)$ from $\dot{\alpha}$ and $\alpha(t)$ data. The interpretation of $f(1-\alpha)$ is the essential link in this method between the experimental data and the functions.

Physical interpretations

The function $f(1-\alpha)$

Solid-state reactions are complex processes which proceed in several stages. These can be the delocalization or transfer of electrons in chemical bonds (in the case of non-metals), the diffusion of atoms, free radicals, or ions, the desorption

of product molecules when they are in the gaseous phase. the heat transfer to the reaction zone in the case of endothermic reactions. and the formation of a new solid structure (crystalline or amorphous) if one of the products is in the solid phase. The last step may often be further differentiated into nucleation. growth of nuclei (at velocities which depend on sizes of nuclei) [1] and sometimes the collapse of the lattice from a transitory one to the equilibrium structure [2]. Irrespective of the details of reaction mechanisms. however. under a given set of circumstances (T, x, sample history etc.) one of the stages will be the slowest. It then acts as the rate limiting step of the reaction, and it will determine the kinetics i.e.. the rate law in (1).

Further. a solid-state reaction has, in contrast to a homogeneous reaction whose progress is independent of spatial coordinates. an additional controlling factor. namely topochemistry. This refers to the geometrical shape of the solid reactant and. in different cases. to its free surface area. its defect structure. the thickness of the product layer if solid. or to the product-reactant boundary, etc.

The function $f(1 - x)$ reflects the nature of the rate-limiting step and the topochemistry of the reaction. It may accordingly depend on certain sample conditions. such as whether the sample has been pre-irradiated or bleached. and whether the sample is in the form of a powder, or a large single-crystal of a different shape from the crystallites. It will vary in several ranges of T if in each of them a different elementary step becomes rate-limiting. as occurs in the decomposition of potassium azide [3]. At a given temperature. it may also change in different ranges of x. due to the switching of the rate-limiting step or topochemical changes. This happens, for instance. in the oxidation of zirconium [4] and in most decomposition processes [1]. An extreme case is the decomposition of ammonium perchlorate which, in the two temperature regimes below and above $620K$, has entirely different reaction mechanisms and in fact yields different reaction products [5]. In such cases there may be competing paths for the chemical reaction or it may in fact be followed by another chemical reaction whose 'onset temperature' is higher. In all possibilities. however, $f(1 - x)$ should be the same for a given x independent of T (within a range) if it is to have more than only an empirical significance.

In Table 1 we have collected together the more common forms of $f(1 - x)$ which have been used in the literature. and the corresponding integrated forms $\int_0^t dt\, \dot{x}/f(1 - x) = \int_0^x dx/f(1 - x) \equiv F(x)$. Note that $F(x) = K\,(t - t_0)$ if the range of x for which it becomes applicable starts at $x = x(t_0)$. Also. for simplicity hereafter we write K for $K(T)$.

In many reactions. such as most decompositions and dehydrations, the rate-limiting step takes place at the interface between different phases as in sublimation. The speed at which the interface moves into the reactant is (at a given temperature) then either a constant, or a unique function of the interfacial area. This area therefore. from the kinetic point of view, plays the same role as that of concentration in homogeneous reactions. If the speed is constant, then the theoretical significance of $f(1 - x)$ is clear: it gives the area expressed as a fraction of the original area at $x = 0$. This is the case of a reaction controlled by the movement of a coherent phase-boundary and listed as F, G and H in Table 1. In this situation, the explicit form of $f(1 - x)$ depends on the geometry of the reacting system, though generally it is a decreasing function of x or at most constant.

If the reaction consists of the formation of compact nuclei of a solid product at localized places in the reactant followed by their relatively rapid growth. then, to express the total interfacial area, $f(1 - x)$ is derived from the laws of nucleation and growth. This is the situation when the reaction is autocatalytic [13]: reactant molecules at a reactant-product interface react in preference to those at a reactant-'vacuum' surface. The preference is due to the existence of microstrains in the reactant at the interface, or due to the electrochemical potential of the product phase when the rate-limiting step is a redox process. The various possible forms of

$f(1 - x)$ for an autocatalytic reaction are listed in Table 1, A to E. Note that they have the general form $f(1 - x) = x^p(1 - x)^q$. In A, B and E, q is zero and x increases monotonically with x. Such a situation is most unlikely to last up to $x = 1$. These types of $f(1 - x)$ therefore may apply only to the acceleratory part, if it is present in the x-time curve and which will usually be followed by a decay part. In C and D, q is non-zero and these types give sigmoid-shaped curves. The inflexion point occurs at $x' = p/(p + q)$, as can be seen at once from the condition $\ddot{x} = 0$. It is thus kinetically feasible for them to fit the complete experimental curve. There are, however, physical grounds to consider that even they should be used to analyze only the acceleratory period [1].

In other reactions the rate-limiting step is not confined to, or does not only occur at, the reactant surface. For instance, in the unimolecular-decay type of reaction, all molecules whether on the surface or in the bulk have an equal probability per unit time of reacting. This is the case when the change from the reactant to the solid product phase involves little re-arrangement of the reactant atoms. The reaction has homogeneous mechanism and thus a true reaction order of one, i.e. $f(1 - x) = 1 - x$. Many decomposition reactions tend to this

Table 1

The common types of solid-state reaction

Reaction	
Autocatalytic	Power-law nucleation and growth at constant speed: A
	Linear branching chain of nuclei, no overlap during growth: B
	Branching-chain nucleation, interference during growth: C
	Random nucleation, growth accompanied by ingestion of nuclei: D
	Instantaneous nucleation, size-dependent growth: E
Phase-boundary controlled decay	1-dimensional: F
	2-dimensional: G
	3-dimensional: H
Unimolecular decay: I	
Diffusion-controlled	1-dimensional: J
	2-dimensional: K
	3-dimensional: L

	$f(1 - x) = \dot{x}/K$	$F(x) = Kt$	m [i]	Reference
A	$x^{1-1/n}$	$nx^{1/n}$	$\approx 1.27n$	[6]
B	x	$\ln x - C(T)$	[ii]	[7]
C	$x(1 - x)$	$-\ln\{-(1 - 1/x)\} - C_0$	[ii]	[8]
D	$\{-\ln(1 - x)\}^{1-1/n}(1 - x) \simeq$	$n\{-\ln(1 - x)\}^{1/m}$	n	[9, 10] [iii]
	$\simeq x^{1-1/n}(1 - x)^b$			
E	$x^{3/2}$	$2(x_0^{-1/2} - x^{-1/2})$	[ii]	[11]
F	1	x	1.24	[3]
G	$(1 - x)^{1/2}$	$2\{1 - (1 - x)^{1/2}\}$	1.11	
H	$(1 - x)^{2/3}$	$3\{1 - (1 - x)^{1/3}\}$	1.07	[12]
I	$1 - x$	$-\ln(1 - x)$	1	[13]
J	$1/x$	$x^2/2$	0.62	[14]
K	$1/\{-\ln(1 - x)\}$	$x + (1 - x)\ln(1 - x)$	0.57	[14]
L	$1/\{(1 - x)^{-2/3} - (1 - x)^{-1/3}\} \simeq$	$3\{1 - (1 - x)^{1/3}\}^2/2$	0.54	[15] [iv]
	$\simeq 3(1 - x)^{1/3}\{-\ln(1 - x)\}$;			
	$1/\{(1 - x)^{-1/3} - 1\} \simeq$	$3\{1 - (1 - x)^{2/3}\}/2 -$	0.57	[16] [iv]
	$\simeq 3/\{-\ln(1 - x)\}$	$- x$		

i) $\text{Log}\{-\ln(1 - x)\} \simeq \text{Constant} + m \log t$, $0.15 < x < 0.5$

ii) Plot of L.H.S. in i) against $\log t$ distinctively concave upwards; C_0 and x_0 are constants while $C(T)$ is function of temperature

iii) $b = 0.774, 0.700, 0.664, 0.642, \ldots, 0.556$ for $n = 2, 3, 4, 5, \ldots, \infty$

iv) Alternative derivations; we have obtained the approximate forms of $f(1 - x)$ by expanding into series $(1 - x)^{-2/3}$ and $(1 - x)^{-1/3}$ to second order in x; resulting error $\simeq x^2/6$ ($<10\%$ for $x < 0.8$)

limit at high α values. Another example is when the rate-limiting step is the migration of product ions along the dislocation network to form additional growth nuclei at dislocation nodes [17]. This leads to $f(1 - \alpha) = \alpha$, the same form as for branching nuclei [7]. The slow process of 'ageing' in some explosives when they are stored at room temperature may be by such a nucleus-chain mechanism. A third category consists of reactions controlled by the diffusion of reactants across a product layer which is solid. The diffusion may proceed uniformly through the bulk of the layer and is thus structure-insensitive, or preferentially along its gross lattice imperfections arising from product-reactant mismatch. In the case of uniform diffusion, the speed at which the product-reactant interface moves is a function only of the product thickness (and temperature), and the appropriate forms of $f(1 - \alpha)$ are included in Table 1 as J, K and L. The oxidation of metals often follows diffusion-controlled kinetics; in sheet form these tarnish according to the parabolic law $\alpha^2 \times t$. Exceptions are those metals in Groups Ia and IIa of the Periodic Table. Excluding beryllium, they all form oxide layers which are porous, so that the atoms of the metal do not have to diffuse through a coherent layer before coming into contact with oxygen.

The function $K(T)$

It is almost always the case that the temperature-dependent part of (1) can be represented successfully by: —

$$K(T) = K_{\alpha} \exp\left(-E/kT\right) \tag{2}$$

in which k is Boltzmann's constant, and the macro-kinetic constants E and K_{α} do not depend on T (within the range), though usually they take on different values when $f(1 - \alpha)$ changes.

If it is established that the reaction is rate-limited by a diffusion or migration process, the interpretation of $K(T)$ is complicated, but obviously it is proportional to the corresponding transport coefficient, which in general is an exponential function of T. An over-simplified theory for the situation of uniform one-dimensional diffusion gives $K(T) = (S/V_0)^2 D(T)$, where S is the interfacial area, V_0 the initial volume of the reactant, and $D(T)$ the diffusion coefficient (cf. [19]).

For a single-solid-reactant reaction which is controlled by a surface process, on the other hand, the simple theory of Shannon [18] is often successful. This theory is a generalization of the Polanyi — Wigner equation. Assuming the existence of some activated complex, which as a transition state can be treated in thermodynamic equilibrium with the reactant, he related the pre-exponential factor K_{α} to the rotational and other internal degrees of freedom of a reactant molecule in addition to the vibrational ones. Following Shannon we can set: —

$$K_{\alpha} = (kT/h) \exp\left(\Delta S^{\ddagger}/k\right) \quad \delta S_0/V_0 \tag{3}$$

and
$$\exp\left(-E/kT\right) = \exp\left(-\Delta H^{\ddagger}/kT\right). \tag{4}$$

Here the mean-frequency factor kT/h containing Planck's constant is usually in the region of $10^{13}\,s^{-1}$ (see below). $\Delta S^{\ddagger}$ and $\Delta H^{\ddagger}$ are respectively the entropy and the enthalpy of formation of the transition complex, δ is the thickness of one monolayer and V_0 the initial volume of the reactant, and $S_0 f(1 - \alpha)$ gives the free surface or the product-reactant interface area when the degree of conversion is α. (Strictly speaking, it has been assumed that the reaction proceeds isobarically).

Note that in this interpretation the empirical quantity K_{α} contains the surface-to-volume ratio and so depends on the sample geometry. Also, it is apparently proportional to T. (In gas reactions, the collision theory gives $K_{\alpha} \propto T^{\frac{1}{2}}$.) In our opinion, however, if the vibrational modes are being considered then only at low temperatures will the peak distribution of phonon frequencies lie at kT/h. For most substances (with the exceptions of Be, Cr and diamond) the Debye temperature θ_D is less than 500K, so that the frequency factor should stay as $k\theta_D/h \lesssim 10^{13}\,s^{-1}$ for all likely experimental temperatures.

The factor $\exp(\Delta S^{\ddagger}/k)$ may alternatively be written in terms of partition functions as $Q^{\ddagger}/Q$, which can be determined from spectroscopic data [20]. In most cases $\Delta S^{\ddagger}$ cannot be larger than the reactant entropy of melting, and $\exp(\Delta S^{\ddagger}/k)$ comes out normally between unity and 10^4. Occasionally $\exp(\Delta S^{\ddagger}/k)$ is found to be less than unity, as is the steric factor in gas reactions. Such a negative value of $\Delta S^{\ddagger}$ means that the activated complex is more ordered than the reactant (e.g. [21]). Experiments on some decomposition reactions have given K which are abnormally high in comparison to the theoretical values of (3). Hypotheses put forward to explain such discrepancies include co-operative activation [22], proton-delocalization [23], and a mobile layer of molecules on the reactant surface [18].

Kinetic analysis

Current practice

In determining the kinetics one wishes to find K, E and $f(1 - x)$ or equivalently $F(x)$ so that the reaction velocity can be predicted at any given T and x. This is commonly done by analyzing a set of $x(t)$ or equivalently $\dot{x}(t)$ values obtained by monitoring a number of samples reacting isothermally at a number of temperatures. The consistency of the K_x and E values with $f(1 - x)$ should as far as possible be assessed, and correlated with, for instance, microscopy.

A quick method of calculating E was used by Haynes and Young [24]. Consider a set of (x, t) curves which have been found to be isomorphic. For any two curves (x_1, t_1) and (x_2, t_2) corresponding to temperatures T_1 and T_2 respectively, one can write

$$F(x_1) = t_1 K_\tau \exp(-E/kT_1)$$

$$F(x_2) = t_2 K_\infty \exp(-E/kT_2) .$$

$$(5)$$

By choosing points corresponding to the same x on the two curves so that $F(x_1) = F(x_2)$, E can be evaluated by plotting $\ln t$ vs. $1/T$. On the other hand, to determine $F(x)$ often a trial-and-error method is resorted to. Conflicting forms of the function have sometimes been asserted by several authors for the same material, like NH_4ClO_4 (see [25]) and KM_nO_4 (see [26]).

A conventional way of superimposing isothermal curves is to convert them into 'reduced-time plots' by individually scaling their t-axis with the factor $1/\tau_i$, where τ_i is the time when $x = 0.5$ on the i-th curve. In this way $K(T_i)$ is absorbed into each scale factor and all $(x, t) = (0.5, 1)$ points coalesce, while other $x(t)$ points may be plotted out to see if the curves are indeed isomorphic. Sharp et al. [27] tabulate the theoretical values of x against t/τ for some of the $F(x)$ shown in Table 1. They propose that by comparing experimental data with such master values the correct $F(x)$ can be identified.

The above method may, however, result in ambiguity due to a number of aspects. Experimental data contain random errors, but no simple statistical analysis can be applied to the identification criterion it employs because no straight-line graphs are involved. Additionally, a general problem for all isothermal experiments is the zero-time uncertainty. The finite time taken by the sample to reach the designated temperature may be negligible relative to τ, yet may affect the comparison with the tabulated values [28]. Moreover, $F(x)$ may change in different regimes of the $\alpha(t)$ curves, as mentioned earlier.

A new method

Here we suggest a step-by-step approach to determine $F(x)$. It was noted by Hancock and Sharp [28] that for many forms of $F(x)$, the plot of $\log[-\ln(1 - x)]$ vs. $\log t$ is almost linear if x is restricted to between 0.15 and 0.5. Using a computer program to generate artificial values and their log-ln plots, we have found

this true for all the theoretical forms listed in Table 1, with the exception of B, C and E. The slope in each case is listed there under the Column 'm'.

Obviously a log-ln plot is not very sensitive. If we were to rely solely on it to discriminate between the functional forms of $F(x)$, the experimental data would have to be of the highest quality. A slightly more sensitive way is to plot $[-\ln(1 - x)]^{1/m}$ vs. t, but then m can only be obtained iteratively. Fortunately, m does differ significantly between different groups of $F(x)$, and the final discrimination is easily achieved by a further graphical step. There are three possible situations for this second step: —

1. $m \approx 2$ or log-ln concave upwards

It will be seen from Table 1 that this situation suggests an autocatalytic reaction, for which $\dot{x} = K x^p (1 - x)^q$ for certain p and q. From the experimental data of $\dot{x}$ and x, one can then do a least-squares fit on the graph of $\Delta \log \dot{x} - \Delta \log x$ against $\Delta \log(1 - x) - \Delta \log x$, and find p from the y-intercept and q from the slope. Here $\Delta \log \dot{x} \equiv \log \dot{x}(t_1) - \log \dot{x}(t_2)$, etc.

For an $\dot{x}$ expression of this form, one has $p(1 - x') = qx'$, where x' is the value at maximum $\dot{x}$. Using this relation to reduce the number of unknown parameters to one, one can use a simpler graph to determine p and q [26]. However, the calculated values of p and q are then subject to the accuracy of x' and, more fundamentally, the possibility that p and q may change from one range of x to another is not allowed for. As mentioned above, those types of $f(1 - x)$ in which $q = 0$ represent the acceleratory period which, in general should be followed by a decay period governed by a different form of $f(1 - x)$.

2. $m \approx 1$

The reaction is either phase-boundary controlled or unimolecular, and $\dot{x} = K(1 - x)^s$, as seen in Table 1. One then draws the graph of $\log \dot{x}$ against $\log(1 - x)$ to find r, the apparent reaction order.

3. $m \approx 0.5$

The reaction is diffusion controlled (see Table 1). One has to test separately whether $x(t)$ is parabolic (the diffusion is in one dimension), or $-\dot{x}\ln(1 - x) = K(1 - x)^s$ with $s = 0$ (two dimensions) or $s = 1/3$ (three dimensions).

The correlation coefficient in the least-squares fit serves, by measuring the linearity of the $\dot{x}$ graph, as a quantitative indication of the confidence to be attached to the identified form of $f(1 - x)$. It may be that p and q, r, or s change once or twice as the reaction proceeds from beginning to completion, but the $\dot{x}$ graphs will show it by displaying several linear segments. If however, a part of the graph say from (x_1, t_1) to (x_2, t_2) is non-linear, then $F(x)$ has changed to a form in another group. The first step should then be repeated for that part: $\log[-\ln(1 - [x + x_1] / [1 - x_1])]$ is plotted vs. $\log(t - t_1)$ for x between $x_1 + 0.15(x_2 - x_1)$ and $x_1 + 0.5(x_2 - x_1)$, followed by one of the above three alternative procedures. On the other hand, if a good fit is found with values of p and q, r, or s that are not in Table 1, the experimenter should assess whether theoretical justification can be provided. In this way new rate laws may be identified.

Confirmation is carried out by plotting the selected functional form or forms on top of the experimental curve. A slight misfit in the very early part (≈ 1 minute, depending on the sample size and the environment) may be attributed to thermal lag-time and ignored. The $\dot{x}$ graphs give K, and from a set of K values at different temperatures K, and E can be determined. Note that the determination of these macro-kinetic constants depends on the form of $f(1 - x)$ chosen, as it should be.

It may be added that we see it an immediate possibility to have full automation in the acquisition and processing of data in thermal analysis experiments. The hardware can be under the control of microprocessors or dedicated minicomputers, and their output would go into a computer or the same minicomputer. A computer program can then reduce the data to $x(t)$ or $\dot{x}(t)$ curves, and further analyse
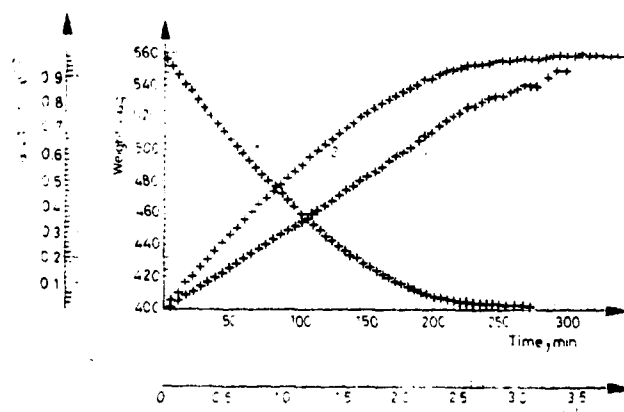
Fig. 1. Decomposition of a single crystal of AgN_3 at 551 K; 1. Thermogravimetric data. 2. x-time curve. 3. $1 - (1 - x)^{1/4}$ vs. time.
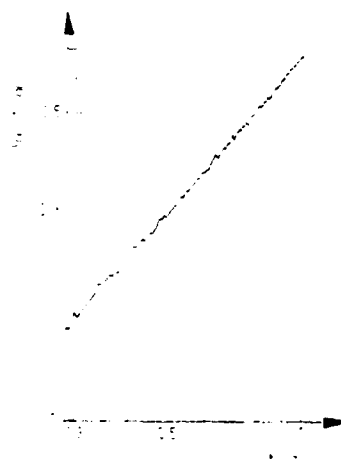
Fig. 2. Log-ln plot

the curves to identify $f(1 - x)$ and so calculate K_x and E, according to the method proposed here. Nevertheless, the physical interpretation of these results by the experimenter remains the crucial step.

The method has been applied to investigate the kinetics of slow thermal decomposition in silver azide single crystals using thermogravimetric data. Curve 1 in Fig. 1 is a typical experimental curve of weight loss against time t, and Curve 2 is the corresponding reduced-time plot of x vs. t/τ. In Fig. 2 we plot log[−ln(1 −

Fig. 3. γ graph
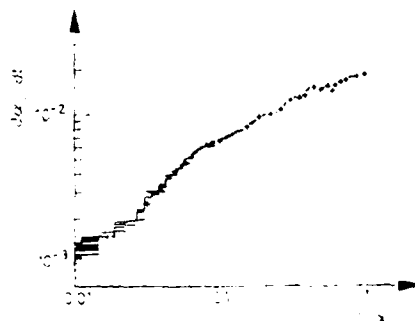
— α)] vs. log(t/τ) for 0.15 < α < 0.5, obtaining essentially a linear graph of slope ≈1.1. The decomposition of AgN₃ therefore appears to be phase-boundary controlled or unimolecular. Accordingly, we draw in Fig. 3 the graph of log $\dot{\alpha}$ vs. log(1 — α). It shows that between 1 — α = 1 to 0.1, $\dot{\alpha} = K(1 — α)^\frac{1}{2}$ with the correlation coefficient among the data points better than +0.9. Indeed, the plot of 1 — (1 — α)¹ vs. t (Curve 3, Fig. 1) is a good straight line, with a correlation coefficient of +0.99 for 0.1 < α < 0.9. The decomposition is thus of the contracting cylinder type. We have also obtained K, and E, and found that their interpretation in terms of Eqs (3) and (4) leads to a plausible physical picture. Further details are given in a separate paper devoted to the mechanism of the thermal decomposition of AgN₃ [30].

In a second paper [29], we discuss the analysis of dynamic kinetic data which are easily obtained from modern thermoanalytical instruments.

Conclusion

We have described a systematic method for determining the kinetics of solid-state reactions from isothermal data. It may be stressed once more that whenever possible a judgement should then be made on the consistency of the K_∞ and E values with the implication of $f(1 — x)$ regarding the likely mechanism of the reaction.

*

References

1. D. A. YOUNG, Decomposition of Solids, Pergamon, Oxford, 1966.
2. J. SAWKILL, Proc. Roy. Soc. London, Ser. A 229 (1955) 135.
3. P. W. M. JACOBS and F. C. TOMPKINS, ibid., Ser. A 215 (1952) 265.
4. V. T ROZENBAND and E. A. MAKAROVA, Combustion Expl. Shock Waves, 12 (1977) 601.
5. A. K. GALWAY and P. W. M. JACOBS, Proc. Roy. Soc. London, Ser. A 254 (1960) 455.
6. W. E. GARNER and L. W. REES, Trans. Faraday Soc., 50 (1954) 254.
7. H. R. HAILES, ibid., 29 (1933) 544.
8. E. G. PROUT and F. C. TOMPKINS, ibid., 40 (1944) 488.
9. M. J. AVRAMI, J. Chem. Phys., 7 (1939) 1103; 8 (1940) 212; 9 (1941) 177.
10. B. V. EROFEEV, Compt. Rend. Acad. Sci. U.S.S.R., 52 (1946) 511.
11. P. W. M. JACOBS and A. R. T. KUREISHY, Trans. Faraday Soc., 58 (1962) 551.
12. S. ROGINSKY and E. SCHULZ, Z. Phys. Chem., A138 (1928) 21.
13. J. Y. MACDONALD and C. N. HINSHELWOOD, J. Chem. Soc., 127 (1925) 2764.
14. J. B. HOLD, I. B. CUTLER and M. E. WADSWORTH, J. Am. Ceram. Soc., 45 (1962) 133.

15. W. Jander, Z. Anorg. Allgem. Chem., 163 (1927) 1.
16. A. M. Ginstling and B. I. Brounshtein, J. Appl. Chem. U.S.S.R., 23 (1950) 1327.
17. R. A. W. Hill, Trans. Faraday Soc., 54 (1958) 685.
18. R. D. Shannon, ibid., 60 (1964) 1902.
19. W. Nernst, Z. Physik. Chem., 47 (1904) 52.
20. F. N. Cagle and H. Eyring, J. Phys. Chem., 57 (1953) 942.
21. K. J. D. Mackenzie*and R. K. Banerjee. Trans. J. Brit. Ceram. Soc., 77 (1978) 88.
22. W. E. Garner, Nature, 144 (1939) 287.
23. J. J. Fripait and F. Toussaint, J. Phys. Chem., 67 (1963) 30.
24. R. M. Haynes and D. A. Young, Disc. Faraday Soc., 31 (1961) 229.
25. J. N. Maycock and V. R. Pai Verneker, Proc. Roy. Soc. London, Ser. A 307 (1968) 303.
26. W. L. No, Aust. J. Chem., 18 (1975) 1169.
27. J. H. Sharp, C. W. Brindley and B. N. Narahari Achar, J. Am. Ceram. Soc., 49 (1966) 379.
28. J. D. Hancock and J. H. Sharp, ibid., 55 (1972) 74.
29. T. B. Tang and M. M. Chaudhri, submitted.
30. T. B. Tang and M. M. Chaudhri, Proc. Roy. Soc. London, Ser. A 369 (1979) 83.

SECTION 5

ANALYSIS OF DYNAMIC KINETIC DATA FROM SOLID-STATE REACTIONS

Tong B. Tang and M. M. Chaudhri

Physics and Chemistry of Solids, Cavendish Laboratory, Madingley Road, Cambridge U. K.

The kinetics of heterogeneous reactions, involving one reactant in the solid phase, usually follow the law $\dot{\alpha} = K_\infty \exp(-E/kT)f(1-\alpha)$, where α is the degree of conversion of the solid, and K_∞ and E are the kinetic constants. A critical examination is given of the various methods which are currently used to analyse dynamic experimental data. The limitations of these methods and their insensitivity to the form of $f(1-\alpha)$ are pointed out. An alternative approach free from these limitations is suggested. In this, $f(1-\alpha)$ is determined from isothermal experiments, and then the dynamic data are accurately analyzed to obtain the values of the kinetic constants. A case study is given to elucidate the applicability of the approach.

There are many reactions of interest in which one of the reactants is in the solid phase. These reactions can be classified variously as decomposition, dehydration, calcination, dehydroxylation, reduction, polymeric inversion and degradation, oxidation etc., and they occur in a wide range of substances including ceramics, explosives and biological materials. The dynamic method of studying their kinetics involves measuring the reaction rates under conditions of a continuous temperature change.

Originally proposed by Skramovsky [1], the dynamic method is becoming increasingly popular, especially with the development of differential thermoanalytical techniques like DSC and DTA. Since the initial temperature can be chosen so that the reaction rate is relatively insignificant to begin with, it does not suffer from zero-time inaccuracy—a problem which exists in isothermal experiments where the temperature is raised rapidly and then held constant at a particular value. A further advantage is that, provided the dynamic data have been unambiguously and correctly analyzed, any changes in the kinetic constants will not be over-looked even within small temperature intervals. In contrast, the isothermal method only provides values averaged over discrete points in temperature. Also, when the method of analysis used is such that the kinetic constants are calculated from each dynamic curve then very few samples are required; only a milligram or so of the material is

needed for its thermal characterization. If many runs are indeed carried out, differences between individual samples can be determined. The last two advantages are particularly useful in single crystal work.

On the other hand, intrinsic differences should be carefully distinguished from the effects of experimental conditions. In the first case literature data have shown

that experimental parameters such as sample mass [53] and shape, particle size in the case of powder samples, and ambient atmosphere (or vacuum) can affect significantly the calculated values of kinetic constants (see [2]). If this happens, then whenever possible the empirical results should be extrapolated to refer to a 'standard' set of experimental conditions. Secondly, the heating rate very often affects the shape of the dynamic curve obtained, but discussion will be deferred to the next section. Lastly, the very fact that temperature is now a variable, in addition to time, complicates the analysis of data. If due care is not taken, either inaccurate or totally misleading values are obtained. In fact, a survey of the literature reveals several instances of high-quality experimental data being mis-interpreted by methods beyond their ranges of validity. In this paper, we first describe the various methods and point out their limitations. We then defend the approach in which use is made of both isothermal and dynamic experiments. The analysis of isothermal data yields $f(1-x)$ (as defined below) unambiguously and, knowing $f(1-x)$, one can calculate individual values of the kinetic constants from each set of dynamic data. We may mention that, historically, isothermal experiments were the only ones employed in the pioneering age in the twenties and thirties, when solid-state reactions began to be studied from the modern point of view, as distinct from that of Langmuir, Nernst and Tammann.

Kinetic equation

As discussed elsewhere [3] the kinetics of a reaction proceeding isothermally can usually be described by the empirical relation:

$$(\dot{x})_{\text{isothermal}} = K_r f(1-x) \exp(-E/kT). \tag{1}$$

Here x is the fraction of the solid reacted, k Boltzmann's constant, T the temperature, and $f(1-x)$ and the constants K_r and E are characteristic to the reaction. The function $f(1-x)$ may change in different ranges of x but is, for a given x, independent of T, at least within a range of T. K_r and E should be the same for the same $f(1-x)$. If the rate-controlling step of the reaction occurs on the reactant-free surface or on the reactant-product (solid) interface, then K_x will contain the surface-to-volume ratio. In other words, the reacting system should really be normalized per unit area rather than per unit size, and K_r be given in units such as molecules $s^{-1} m^{-2}$.

Some authors have questioned the general validity of (1) on various grounds [4-7]. However, in the literature (1) is almost always successfully fitted to experimental data. Indeed, this empirical relation can be given mechanismic jutification (see [3]).

In dynamic experiments, also, it is commonly agreed that (1) may be adapted to describe the reaction rate:

$$\dot{x} = K_r f(1-x) \exp[-E/kT(t)] \tag{2}$$

$T(t)$ is controllable by the experimenter. Some temperature programs offer the mathematical advantage that $\exp[-E/kT]/\dot{T}$ can be integrated analytically (see later discussion on integral methods of data analysis). Examples are the hyperbolic program where $1/T = A - Bt$, i.e. $\dot{T} = BT^2$ [8, 9]; a parabolic program in which $AT^2 + BT - C = t$, i.e. $1/\dot{T} = 2AT + B$, with $B = AE/K$, by iteration [10]; and an exponential program so that $\dot{T} = \exp(-B/T)$ with $B \simeq E/k$ [10]. For the sake of experimental convenience, however, the arrangement is usually that $\dot{T} = \phi$ (A, C and ϕ represent constants in a particular run of experiment).

However, it has been taken by some authors who object to (2), that

$$d\alpha = \left(\frac{\partial\alpha}{\partial t}\right) dt + \left(\frac{\partial\alpha}{\partial T}\right) dT + \left(\frac{\partial\alpha}{\partial\phi}\right) d\phi \qquad (3)$$

where $\left|\frac{\partial\alpha}{\partial t}\right|_{T,\phi} \equiv (\dot\alpha)_{isothermal}$. The argument is then that (2) is seen to be inadequate even in the case of $d\phi = 0$, since the second term on the R.H.S. of (3) is nonzero but left out in (2): see e.g. [11, 12]. It has further been proposed [13], by a derivation starting from (3), that (2) is correct only if it includes the extra factor

$$[1 + (1 - T_0/T)E/kT]$$

in which $T_0 \equiv T(0)$. But we hold that (3) is unsound. Given t, T and ϕ, α is not uniquely determined and therefore not a function of these system variables: $\Phi d\alpha > > 0$, as α cannot decrease even for negative dT and $d\phi$! Nevertheless, the inexact differential $d\alpha$ can be integrated, if the dynamic process can be treated as the limiting case of a series of time intervals, during which the reaction proceeds isothermally according to (1) but at the end of each of which T is altered, in a time so short that during it the sample is unchanged. Along this path P the result is easily obtained [14]:

$$\int_0^\alpha \frac{d\alpha}{f(1-\alpha)} = \int_P K dt = \frac{K_\alpha}{\phi} \int_{T_0}^T \exp(-E/kT) dT \qquad (4)$$

where $K = K_r \exp(-E/kT)$. We must emphasize that (4) is not logically self-evident, as is sometimes implied [14] or argued by mathematical operations based on the presumption that $\alpha = \alpha(T, t)$ [15]. Rather, it comes from the assumption that the reaction under study involves no slow processes, so that $\dot\alpha$ depends only on the present values of α and T ($\dot\alpha$ is a function of state), but not on the history of the reacting system (c.f. [16]). Only by this assumption (absence of memory effects) can the dynamic process be treated as P. (Experimentally, a temperature program with temperature jumps, which approximates P, has been realized on a thermo-balance interactively controlled by computer [17].) Equations (2) and (4) are of course equivalent. Their validity has also been shown by 'rational' thermodynamic arguments, in which the functional relation $\dot\alpha = g(t, \dot Kt)$ is regarded as the 'constitutive equation' characterizing the reaction system [18]. In a new direction, the possibility has been suggested [64] that solid-state reactions may be studied by far from equilibrium thermodinamics.

On the other hand, experience shows that apparently (4) is not always followed exactly. Consider a reaction being investigated by a series of experiments conducted at different heating rates ϕ but with the same initial temperature T_0. In (4) we see that the R.H.S., for a given upper temperature limit T, is directly proportional to $1/\phi$. Plots of the L.H.S. vs. T should therefore all have the same shape. It may happen, however, that increasing departure from isomorphism is seen when experimental data obtained at higher ϕ are so analyzed. The most probable explanation is that the temperature change is too fast, causing the temperature distribution in the sample to become significantly non-uniform. In fact, thermal equilibrium is an underlying assumption when (4) is derived above: without it $\dot\alpha$ will depend on the thermal history of the reacting system.

Other factors may also be at work. The reaction rate may be sensitive to the structure of the reactant, and a higher ϕ can enhance the defect density or change the activation energy of reaction at a defect site [19]. In branched-chain reactions, the speed of the progressive accumulation of active centres may vary with the rate of change in temperature [20]. If the reaction is a surface process, the distribution

of reaction 'centres' among corners, edges or faces of the sample may change with ϕ [21]. It may also be that the chemical system under study has multiple reactions proceeding concurrently in it, and they have different E [22]. All these variations in E may be accompanied by changes of K_x in the same direction. Because of this coupling, a linear relation between E and $\log K_x$ is sometimes observed. Called the 'compensation effect', this phenomena does not necessarily mean, as was suggested [4], that the Arrhenius expression in the R.H.S. of (4) is invalid. In all these cases, by varying ϕ the experimenter can, in fact, gain additional insights into the mechanism of the reaction, or distinguish between the competitive reactions in the reacting systems (a situation usually, though not always, indicated by the presence of multiple peaks in the $\dot{\alpha}$ curves). This is possible if the method of data analysis employed is such that K_x and E are determined from a single $\dot{\alpha}$ or α curve, rather than from data at a number of heating rates. The method we suggest will be of this type.

It may also happen that in (2) $K_x \propto T$, so that it cannot be taken outside the integral sign in (4). Indeed, modifications have been suggested of some methods of data analysis (those that assume a reaction order for the reaction) to take this extra temperature dependence into consideration [23]. However, even when theoretically required, the correction may for practical purposes be ignored, unless E is small or temperatures used are very high (d $\ln K/dT = [E + kT]/kT^2$). Likewise, any slight temperature dependence of E can usually be neglected. Furthermore, irrespective of this or the above complications the form of $f(1-\alpha)$ in (2) and (4) is not affected. It should be the same as that in (1), on the basis that the dynamic process can be treated as the limiting case of a series of isothermal intervals, as already mentioned above.

Data analysis

Experimentally, $\dot{\alpha}$ or α is obtained by DSC, DTA, TG, DTG, quantitative IR spectroscopy or X-ray diffraction, dilatometry, or measurements of chemi-luminescence, ultrasonic attenuation, dielectric constant, viscoelasticity, thermal or electrical conductivities, or optical reflectivity when changes in these characteristics can be correlated with α. The oldest technique is thermomanometry, in which the pressure of an evolved gas is measured at constant volume, but its use has so far been more popular in isothermal experiments. Many methods of analyzing $\dot{\alpha}$ or α data have been proposed to calculate the kinetic constants E and K_∞ (for a critical review of the earlier work see [24]) and sometimes also $f(1-\alpha)$. Often they were originally formulated with reference to one particular instrumentation, but they may be made generally applicable to all techniques after quantities measured on DSC, DTA, TG instruments etc. are all interpreted in terms of α and $\dot{\alpha}$. On the other hand, their validity does depend on the particular reaction whose data are being analyzed. Their limitations in this respect form the subject of our discussion below. They will be examined in three groups: peak-temperature, integral and derivative methods, in this order. Sophisticated instrumentation systems are coming into use, that incorporate computers to establish baselines or other null settings, to carry out automatic data acquisition, and to let the experimenter interactively analyse the data (e.g. [25]). Such advances do not, however, remove the danger of uncritical choices of the method of data reduction.

Critical examination of current methods

Peak-temperature method

Kissinger [26] considers reactions of the type $f(1-\alpha) = (1-\alpha)^n$. Differentiating (2) with respect to t, and setting the resulting expression to zero, he obtains

$$\dot{\alpha}_m(E/k)(\phi/T_m^2) = \exp(-E/kT_m)n(1-\alpha_m)^{n-1}\dot{\alpha}_m \tag{5}$$

in which m, signifies 'peak' quantities, at the point of maximum $\dot{\alpha}$ where $\ddot{\alpha} = 0$. He next assumes that $n(1-\alpha_m)^{n-1} \simeq 1$; therefore

$$\phi T_m^2 \propto \exp(-E/kT_m) \tag{6}$$

regardless of n, which itself may be calculated from the shape of the $\alpha(t)$ curve. E and k, on the other hand, are obtained by performing a series of experiments at different ϕ. An aspect, which we regard as an inefficiency, of Kissinger's method is that only one point on the curve is used although, in the case where multiple peaks occur signifying that different $f(1-\alpha)$ and E govern different sections of the curve, the method should still be applicable to each peak.

There is, however, an important limitation. The a priori condition that $f(1-\alpha) = (1-\alpha)^n$ is actually valid only in very special circumstances, namely when the rate-limiting step of the reaction is the inward movement at a constant speed of the reactant-product interface, where n is 0, ⅓ or 2/3 for one-, two-, or three-dimensional movement, respectively, or when the reaction is unimolecular so that $n = 1$. Even among these special cases, the other approximation that Kissinger uses is still conditional, since $n(1-\alpha_m)^{n-1} \equiv 1$ only for $n = 1$. When n is ½ or 2/3, this expression varies with α_m approximately as $\Delta\alpha_m\, n(1-n)/(1-\alpha_m)^{2-n} \geq 0.2\, \Delta\alpha_m$, where $\Delta\alpha_m$ is the variation in α_m itself. In the Appendix we show that α_m changes with ϕ in the general case. Hence, when an apparent reaction order exists and is ½ or 2/3, Kissinger's method can lead to a systematic deviation in (6) and thus generate a significant but hidden error in the calculated E and K_r.

If no apparent reaction order exists, then it definitely should not be used, otherwise an approximately linear plot from (6) results in totally misleading values of the kinetic constants. An example is in the decomposition of benzenediazonium chloride: it derives from DTA data a value of E that is 40% lower than the nearly identical values, obtained by applying other methods of analysis to the data from DTA as well as other techniques [27]. Other examples are in the study of lithium aluminium hydride, where the Kissinger values are half of the isothermal result [28], in RDX where it is again 40% lower than all the values calculated by other methods [29], and in urea nitrate, where it is 30% lower [30].

Integral methods

The L.H.S. of (4) is a function of α only and will be denoted by $F(\alpha)$; the R.H.S. can for practical purposes be equated with $\int_0^T K/\phi\, dT$, since in experiments T_0 will be such that reaction velocity is negligible below it, i.e. $T_0 \ll E/k$. In view of these considerations, many authors have proposed different methods of analysing $\alpha(T)$ data.

The temperature integral $\int_0^T \exp(-E/kT)dT$ has no analytical solution. (In the unusual case of a hyperbolic, parabolic or exponential temperature program, on the other hand, $\exp(-E/kT)/\dot{T}$ is integrable.) The numerical values of the integral have been compiled but, being a function of both E and T, are not directly useful unless an iterative solution of (4) by trial-and-error is resorted to. Such an approach has been advocated by Zsakó [31] who considers in particular the cases

of $f(1-\alpha) = (1-\alpha)^n$ with $n = 0, 1/3, 1/2, 2/3, 1$ or 2, when $g(\alpha) \equiv \log \int_0^\alpha \dfrac{d\alpha}{f(1-\alpha)}$

has simple analytical expressions, and by Šatava and Škvára, [32] who generalize the method slightly by tabulating the values of $g(\alpha)$, $0 < \alpha < 1$, for some other forms of $f(1-\alpha)$.

For more efficient approaches, approximations to the integral are necessary. Thus, taking the first two terms in an asymptotic $(u \equiv E/kT \to \infty)$ series of

$$\int_{s}^{u} \exp(-\tau) \frac{d\tau}{\tau^2}$$ Coats and Redfern obtain the linearized relation [33]:

$$\ln\left(F(\alpha)T^{-2}\right) = A - E/k(T^{-1}) \tag{7}$$

where $A = \ln(K, k/E\phi)(1-2kT/E)$ is 'sensibly constant' if the range of temperature ΔT is small. They further assume that $f(1-\alpha) = (1-\alpha)^n$, and so $F(\alpha)$ can be calculated at each (α, T). Plotting (7) for several values of α thus gives E and K, making use of only one set of data corresponding to a single ϕ.

Several cautionary notes should again be made here. The assumption for $f(1-\alpha)$ has already been discussed. Similar to the case of Kissinger's method, results obtained may be wrong and misleading if this functional form is not independently determined beforehand. Thus, in a study on the dehydroxylation of kaolinite [34], straight lines over different ranges of (T^{-1}) are given by (7) for a whole series of values of n, namely, 0, 0.5, 0.667, a and 2. In particular, plots using $n = 1$ and $n = 2$ are almost equally 'good'.

Secondly, the accuracy of the asymptotic approximation is rather low. By comparing its values with tabulated values of the integral [31, 35, 36], we find its relative errors to be $\Delta I/I = 20\%$ at $u = 5$, 5% at $u = 10$, and 1.5% at $u = 20$. Thus, for example, if E is 1 eV, then for an accuracy of 98% the highest temperature reached in the experimental run should not be more than 600 K, a very low figure for most materials though it is higher for larger E. Additionally, expanding A into a power series shows that $\Delta A/A \simeq 2k \, \Delta T/E$, so that at say 2% inaccuracy the range of temperature, ΔT, from which (α, T) points are selected should be less than 100K (for $E = 1$ eV). The total possible deviations in the calculated E and K, are, to first approximation, the sum of the $\Delta I/I$ and $\Delta A/A$. It certainly is unsatisfactory if they are large and yet nowhere mentioned in the calculation.

Other approximations to the temperature integral have been suggested by van Krevelen et al. [37] and by Horowitz and Metzger [38], who made use of certain asymptotic expansions in the vicinity of T_m, the temperature at peak reaction rate. Both have been shown [39] to be even less accurate than the Coats and Redfern approach, and so will be left out in our discussion.

Amongst the integral methods, the best is probably the one due to Ozawa, which requires data at different ϕ but, in it $f(1-\alpha)$ remains completely general. The approximation to the temperature integral is:—

$$\int_{0}^{T} \exp(-E/kT)dT \simeq \frac{E}{k} \, 10^{(-2.32 - 0.457 E/kT)} \tag{8}$$

so that from (4)

$$\log\phi_1 + 0.457(E/k)/T_1 = \log\phi_2 + 0.457(E/k)T_2 \tag{9}$$

where T_1 and T_2 are taken at an arbitrary but identical value of α in the two curves corresponding to heating rates ϕ_1 and ϕ_2. Plotting $\log\phi$ vs. $1/T$ for selected values of α should therefore produce straight lines, the slopes of which give E [40].

Three comments are appropriate here. By comparing (8) with tabulated numerical values, we see that it is 7% out at $u = 10$ or $T = 1170K$, and 3% and less only for $T < 720K$ (if $E = 1$ eV). These errors should be examined before Ozawa's

method is applied. Secondly, the method has been modified [41] to read, in place of (9),

$$\Delta \ln \phi / \Delta T_m^{-1} = 0.457 \, E/k \tag{10}$$

in which $\Delta \ln \phi \equiv \ln \phi_1 - \ln \phi_2$, etc., and m denotes, as before, peak quantities. This relation may be compared with (6) but in general it does not hold since, as shown in the Appendix, x_m varies with ϕ. Lastly, like Kissinger's method, E cannot be determined from data at a single ϕ, and in some cases this may be a disadvantage, as discussed before.

Derivative methods

The derivative methods offer an advantage over those described above in invoking no mathematical approximations. Unfortunately, they use $\dot{\alpha}$ data which, with present instrumentation, tend to be of lower quality whether they are obtained by numerically differentiating the α data or are direct experimental read-outs.

The most straightforward, but as it stands relatively inefficient, of the derivative methods is to write (2) as:—

$$\ln(\dot{\alpha}/f(1-\alpha)) = \ln K_r - E/kT \tag{11}$$

and to substitute different of $f(1-\alpha)$ until a linear plot appears [42]. Later, we shall argue, however, that even this labor omnia vincit approach like all dynamic methods in general, cannot guarantee correct values of E and K_r (nor an unambiguous form of $f(1-\alpha)$ in this specific case), although the labour it involves may be undertaken by the computer.

The earliest derivative method is probably that of Borchardt and Daniels, originally formulated for homogeneous reactions in the liquid phase [43] but later extended to solid-state reactions [44] for which it is now frequently used. The method puts $f(1-\alpha) = (1-\alpha)^n$ into (11), with n given a guessed value, and if a linear plot results then E and K_r are obtained from it. Based on this method, Hauser and Field [45] have developed a computer procedure, in which plots are generated for a series of values of n incremented at discrete steps, and the 'best' one is then selected to yield E, K_r, and n. An attraction of this method is that n can be readily selected by eye. Alternatively, since in this case

$$\Delta \ln \dot{\alpha} / \Delta \ln(1-\alpha) = -(E/k[\Delta T^{-1}/\Delta \ln(1-\alpha)]) + n \tag{12}$$

a plot of the L.H.S. vs. the quantity in the square brackets at once gives E from the slope and n as the y-intercept [47]. If constant $\Delta \ln \dot{\alpha}$, $\Delta \ln(1-\alpha)$, or ΔT^{-1} is selected, Eq. (12) can be further simplified [61]. We have emphasized previously the fallibility in presuming such a convenient form of $f(1-\alpha)$: Ozawa [47] has commented on the possibility that this procedure, and the integral method of Coats and Redfern, may give false values of E and K_r. In addition, since (12) involves the ratios of differences, the quality of data called for is even higher than that demanded alone by the use of $\dot{\alpha}$: experimental data so plotted more often than not show very large scatter. The Rogers and Morris method [48] plots $\Delta \ln \alpha$ vs. T^{-1}, and can be

seen to be the special case of $n = 0$ in (12). An example of the general danger that very linear plots may sometimes appear even if the applied method is not valid is given by Patel and Chaudhri. The Rogers and Morris method was used to analyze DSC data on lead azide, and a straight line results although the calculated E turns out to be 180% larger than the Ozawa value [49]. Conversely, the coincidence of values calculated by various methods need not prove that these methods are all applicable to the case in hand. A counter-example is provided by a DSC study on RDX [29], where the Rogers and Morris value agrees well with other values but the complex decomposition is beyond doubt far from the $n = 0$ type.

On the other hand, Dávid and Zelenyánszki [50] plot $\ln \left| \left| \dfrac{d}{dt}(1-\alpha) \right| / (1-\alpha) \right|$

against (T^{-1}); this amounts to assuming a 'reaction order' $n = 1$. It serves as yet another example of the futility of linear plots, for their method gives such plots for the decomposition of 'a wide range of materials' including calcium oxalate and polyethylene which, most likely, are not of first or any other 'order'.

Some of the integral and derivative methods described in the foregoing have been compared by testing their accuracies on synthesised DTA data (exact as well as with artificial random error) for one E value and temperature range. the reaction considered being of the type with a reaction order [51]. Among the methods not included there is that due to Friedmann [52]. It probably is the most general among the derivative methods. Like Ozawa's procedure. it makes no assumption about $f(1-\alpha)$. although it requires $\dot{\alpha}$ data which. furthermore. have to be at a number of ϕ. Once again. from (2) with $d\alpha/dT \equiv \alpha^T$:

$$\ln(\alpha^T \phi) = \ln(K_\tau f(1-\alpha)) - E/kT. \tag{13}$$

Since $K_\tau f(1-\alpha)$ is identical for the same value of α, taking α^T and the corresponding T from several ϕ one can determine E.

It is our contention that even Friedmann's method has one basic limitation which. more significantly. is shared by all dynamic methods described above. The point in question is that all of them have to presume the constancy of $f(1-\alpha)$ as the temperature is changed. However. since mechanisms of solid-state reactions are generally complicated. there is no general justification for this presumption. though it may be true for particular reactions within specific temperature ranges. An illustration is the case where parallel reaction paths exist. each with values of K_x and E such that a quantitative change of T will lead to a qualitative change in the dominating path. Another case is where the identification of the rate-limiting step depends on T. Methods have been proposed which. by the use of computers. try different forms of $f(1-\alpha)$ in analyzing the dynamic data [53–55]. However. the search is limited to functional forms which are already known.

More importantly. from our own experience with azides we have strong doubts as to the exactness in determining $f(1-\alpha)$ or even its constancy from dynamic data. Likewise. in a study on the dehydration of manganese formate [54] for instance. no unique form of $f(1-\alpha)$ and correspondingly no unique values of E are identified even over appropriately restricted ranges of α, the criterion used being minimum standard deviation in the Arrhenius plot. Further examples are the thermal dehydroxylations of kaolinite [34] and of magnesium hydroxide [56]. We suggest that, in dynamic experiments since data are collected under variable temperature conditions, the change due to $f(1-\alpha)$ is inherently masked by that due to $K(T)$. This pitfall is illustrated in the Figures. Figure 1a shows the graphs of $\alpha(T)$ and its derivative which are generated artificially according to the theoretical equation $\alpha^T = K_\infty$
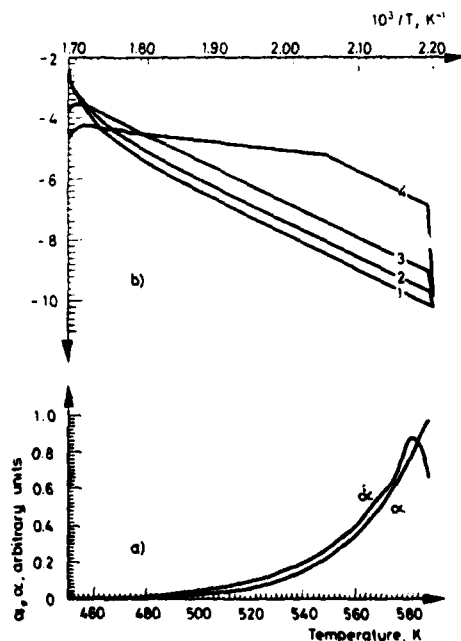

Fig. 1a. Artificial data $\alpha = Kt$. and corresponding $\alpha^T \equiv d\alpha/dT$ data, plotted against T which rises linearly with t

Fig. 1b. Arrhenius plots of: (1) $\alpha^T/3(1-\alpha)^{2/3}$. (2) $\alpha^T/2(1-\alpha)^{1/2}$. (3) α^T. and (4) $\alpha^T/3\alpha^{2/3}$ for the data shown in Fig. 1a

$\exp(-E/kT)$ throughout from $\alpha = 0$ to $\alpha = 1$. The values chosen for K_α and E are 10^8 and leV respectively. Let us now examine how the data generated according to this relation, which is of the type $\alpha = Kt$, will be fitted by different kinetic equations, one of them being the correct one. In Fig. 1b we plot against $10^3/T$ the natural logarithms of the following expressions: —

(1) $\alpha^T/3(1-\alpha)^{2/3}$, i.e. assuming $1 - (1-\alpha)^{1/3} = Kt$: reaction controlled by three-dimensional contraction of phase boundary:

(2) $\alpha^T/2(1-\alpha)^{1/2}$, i.e. $1 - (1-\alpha)^{1/2} = Kt$ type:

(3) α^T: the original assumption; and

(4) $\alpha^T/3\alpha^{2/3}$, i.e. $\alpha = (Kt)^3$: reaction controlled by e.g. three-dimensional growth of existing nuclei.

It is seen that the incorrect $f(1-\alpha)$ in (1) and (2) still give virtually linear plots, with slightly different slopes; interestingly, curve (4) is so misleading as to show two "linear" segments with a seemingly significant transition in between. Experimentally, Guarini *et al.* [57] have noted that it is impossible to ascertain from their DSC data whether the monomerization of 9-Me-10-AcAD has an apparent reaction order of 1, 0.67, or 0.5, in all of which cases E has about the same derived value.

The suggested approach

In the foregoing sections, we have discussed the limitations regarding the applicability of various methods that have been used to analyse dynamic data. In many published works we find that often a number of apparently different methods are used to analyse the same set of data. However, we think that in many cases this procedure is of no real significance, when some of the methods used are mathematically equivalent and therefore lead to the same results, or when some are invalid in the given situation and thus lead to doubtful values. The limitations of the methods express themselves both as discrepancies in the calculated values of the kinetic constants, and sometimes as fortuitous agreements when some of the methods are certainly inapplicable. (An extreme example of the second situation is that, for RDX, the Kissinger value [29] of E is near to that obtained [58] by plotting α vs T^{-1}, a procedure which has absolutely no theoretical justification.) Accordingly, we suggest that the interpretation of dynamic data should as far as possible be based on results from isothermal experiments. A similar approach has been used for studying the dehydroxylation of kaolinite by Achar, Brindley and Sharp [63].

One can unambiguously determine $f(1-\alpha)$ over the whole range of α and over the relevant temperature range, from the independent analysis of individual isothermal curves. A systematic method of efficiently implementing this identification has been proposed by us [3]. It may also be noted that thermoanalytical equipments are equally applicable in isothermal experiments (see e.g. [62]) though they are more often used in the dynamic mode. The identified form(s) of $f(1-\alpha)$ can then be substituted into either (2) or (4). In this way, form the dynamic α or $\dot\alpha$ data one can then determine accurately the non-average and single-sample values of E and K_r: advantages which have been mentioned in the introduction to this paper. Moreover, the values will correspond individually to different heating rates.

We applied this approach to the spinel formation $ZnO + Cr_2O_3 \rightarrow ZnCr_2O_4$. A DTA curve (experimental atmosphere: N_2 at 300 mm mercury) was published in Ishii *et al.* [59], who have also monitored $\alpha(t)$ by chemical analysis when the reaction proceeded isothermally in nitrogen flowing at 50 ml/min, and showed that the isothermal data fit $[1 - (1-\alpha)^{1/3}]^2 = Kt$. We have measured K from the

Table 1

Isothermal data

T, deg. C	K relative units	ln K
800	1	0
900	4	1.4
1000	23	3.1

Table 2

Dynamic data

t, deg. C	α	$\dot{\alpha}$ relative units	$\ln\{\dot{\alpha}[(1-\alpha)^{-1/3} - 1]\}$
700	0.1	2	-2.6
820	0.15	4	-1.4
900	0.2	7	-0.54
1000	0.35	12	$+0.76$

experimental data points at $t = 20$ min in the published isothermal plots. From these values of K, given in Table 1, we calculate a value of 1.5 eV for E.

In Table 2 the values $\dot{\alpha}$ were measured from the published DTA curve whose heating rate was unspecified, and the α values were read off from the (α, T) graph which Ishii *et al.* have drawn presumably by integration. Now, from their analysis of the isothermal data the governing kinetic equation is, in *differential form*, $\dot{\alpha} = K/[(1-\alpha)^{-2/3} - (1-\alpha)^{-1/3}]$. at least within the ranges $800-1000°$ and α from 0 to $\simeq 0.6$ corresponding to $Kt = 0$ to $\simeq 0.07$. The Arrhenius plot of $\dot{\alpha}(1-\alpha)^{-1/3}[(1-\alpha)^{-1/3} - 1]$, for the four data points shown in Table 2, is indeed a good straight line. From the plot we obtain $E = 1.3$ eV. In view of the probable experimental errors and inaccuracies in obtaining data from the published graphs, we consider satisfactory the reasonable agreement between this value and the one calculated from the isothermal data.

Conclusion

Most of the commonly used methods of analyzing dynamic data have been shown to be applicable only under particular conditions. It has been pointed out that to use these methods without *considerations of the range* of their validity can give misleading values of the kinetic parameters. An approach has been advocated in which use is made of both the dynamic and isothermal data: the functional form $f(1-\alpha)$ is determined from the isothermal experiments. This form in conjunction with the dynamic data, gives the values of the kinetic constants.

*

Appendix

We wish to predict how the value of α at peak reaction rate varies with the heating rate ϕ. At $\alpha = \alpha_m$: from (4)

$$\int_0^{\alpha_m} \frac{d\alpha}{f(1-\alpha)} - \frac{K_x}{\phi} \int_{T_e}^{T_m} dT \exp(-E/kT) \equiv F(\alpha_m, \phi, T_m) = 0$$

(14)

and from the fact that $\ddot{\alpha} = 0$

$$f'(1-\alpha_m) - \frac{E}{k} \frac{\phi}{T_m^2} \frac{\exp(E/kT_m)}{K_x} \equiv G(\alpha_m, \phi, T_m) = 0.$$

(15)

Solving the simultaneous equations $dF = 0$ and $dG = 0$, we find

$$\frac{d\alpha_m}{d\phi} = \left(\frac{\partial F}{\partial \phi} \frac{\partial G}{\partial T_m} - \frac{\partial F}{\partial T_m} \frac{\partial G}{\partial \phi}\right) \Big/ \left(\frac{\partial F}{\partial T_m} \frac{\partial G}{\partial \alpha_m} - \frac{\partial F}{\partial \alpha_m} \frac{\partial G}{\partial T_m}\right).$$

(16)

Defining dimensionless quantities $U = E/kT_m$, $\mu \equiv \phi/K_x T_m$, and $I(\alpha_m) \equiv \int_0^{\alpha_m} d\alpha/f(1-\alpha)$, we have the following:

$$\frac{\partial F}{\partial \alpha_m} = \frac{1}{f(1-\alpha_m)}, \qquad\qquad \frac{\partial G}{\partial \alpha_m} = -f''(1-\alpha_m).$$

$$\frac{\partial F}{\partial \phi} = \frac{K_x}{\phi^2} \int_{T_e}^{T_m} dT \exp(-U) = \frac{I(\alpha_m)}{\phi}, \quad \frac{\partial G}{\partial \phi} = \frac{\mu U}{\phi} \exp(U).$$

$$\frac{\partial F}{\partial T_m} = \frac{1}{\mu \exp(U) T_m}, \qquad\qquad \frac{\partial G}{\partial T_m} = \frac{\mu U(2+U)}{T_m} \exp(U). \quad (17)$$

Hence

$$\frac{d\alpha_m}{d\phi} = -\frac{U}{\phi} \frac{h(2+U)I(\alpha_m) - 1}{hU(2+U)/f(1-\alpha_m) - f''(1-\alpha_m)/h}$$

(18)

where $h \equiv \mu \exp(U)$. Incidentally, $dT_m/d\phi$ can be derived in a similar way.

The only case we find reported in the literature, in which α_m is apparently independent of ϕ, is the primary recrystallization of pre-compressed copper [60], where $\alpha_m \cong 0.5$. In all other cases, experiments give changing α_m. We have made a rough check on (18) by taking the case of the decomposition of the explosive RDX [29], for which the Rogers and Morris method gives $E = 2.10$ eV and $K_x = 10^{18.4} s^{-1}$. The reaction is complex, but these representative values are chosen because they correspond to an assumed kinetic equation in which $f(1-\alpha) = 1$. We thus have very simply $I(\alpha_m) = \alpha_m$ and $f''(1-\alpha_m) = 0$. For $\phi = 0.167$ K s^{-1}, α_m is given as 0.62 and T_m as 512K; our calculation shows $d\alpha_m/d\phi \simeq -0.1$ s K^{-1}, a value which compares well with the experimental indication that $\Delta\alpha_m/\Delta\phi = (0.60 - 0.62)/(0.333 - 0.167)$ s K^{-1}.

References

1. S. Skramovsky, Chem. Listy, 26 (1932) 521.
2. J. Simon, J. Thermal Anal., 5 (1973) 271.
3. T. B. Tang and M. M. Chaudhri, ibid. (in press).
4. P. D. Garn, Proc. 4th Int. Conf. Thermal Anal., Budapest, Vol. 1, 1974, p. 25.
5. V. V. Barzukin et al., ibid., 195.
6. A. L. Draper and L. K. Steum, Thermochim. Acta, 1 (1970) 345.
7. D. Krug, ibid., 20 (1977) 53.
8. J. Zsakó, J. Thermal Anal., 2 (1970) 460.
9. J. Simon and E. Debreczeny, ibid., 3 (1971) 301.
10. V. Marcu and E. Segal, Thermochim. Acta, 24 (1978) 178.
11. J. R. MacCallum and J. Tanner, Nature, 225 (1970) 1127.
    J. R. MacCallum, Nature, 232 (1971) 41.
12. M. Murat, A. Fèvre and C. Comel, Proc. 1st Europ. Symp. Thermal Anal., D. Dollimore, ed., 1976, p. 98; J. Thermal Anal., 12 (1977) 429

13. J. NORWISZ, Thermochim. Acta, 25 (1978) 123.
14. E. L. SIMMONS and W. W. WENDLANDT, ibid., 3 (1972) 498.
15. V. M. GORBATCHER and V. A. LOGVINENKO, J. Thermal Anal., 4 (1972) 475.
16. R. M. FELDER and E. P. STAHEL, Nature, 228 (1970) 1085.
17. B. DICKENS and J. H. FLYNN, Proc. 1st. Europ. Symp. Thermal Anal., D. Dollimore, ed., 1976, p. 15.
18. J. ŠESTÁK and J. KRATOCHVIL, J. Thermal Anal., 5 (1973) 193.
19. H. M. C. SOSNOVSKY, J. Phys. Chem. Solids, 10 (1959) 304.
20. V. A. AZATYAN, Kinetics and Catalysis, 18 (1977) 235.
21. F. H. CONSTABLE, Proc. Roy. Soc. London, Ser. A108 (1925) 355; C. HEUCHAMPS and X. DUVAL, Carbon, 4 (1966) 243.
22. I. OZAWA, J. Thermal Anal., 9 (1976) 217.
23. H. R. PETTY, E. T. ARAKAWA and J. K. BAIRD, J. Thermal Anal., 11 (1977) 417.
24. J. H. FLYNN and L. A. WALL, J. Res. Nat. Bur. Std., 70A (1966) 487.
25. A. DOHMAN, A. R. GREGGES and E. M. BARALL II, IBM J. Res. Develop., 22 (1978) 81; Analytical Calorimetry, Vol. 4, R. S. Porter and J. F. Johnson, eds, Plenum Press, New York 1977, p. 1.
26. H. E. KISSINGER, Anal. Chem., 29 (1957) 1702.
27. R. L. REED, L. WEBER and B. S. GOTTFRIED, Ind. Eng. Chem. Fundamentals, 4 (1965) 38.
28. M. McCARTY, JR., J. N. MAYCOCK and V. P. PAI VERNEKER, J. Phys. Chem., 72 (1968) 4009.
29. R. N. ROGERS and L. C. SMITH, Thermochim. Acta, 1 (1970) 1.
30. B. M. BORHAM and F. A. OLSON, ibid., 6 (1973) 345.
31. J. ZSAKÓ, J. Phys. Chem., 72 (1968) 2406.
32. V. ŠATAVA and F. ŠKVÁRA, J. Am. Ceram. Soc., 52 (1969) 591.
33. A. W. COATS and J. P. REDFERN, Nature, 201 (1964) 68.
34. K. J. D. MacKENZIE, J. Thermal Anal., 5 (1973) 5.
35. C. D. DOYLE, J. Appl. Polymer Sci., 5 (1961) 285.
36. J. R. BIEGEN and A. W. CZANDERNA, J. Thermal Anal., 4 (1972) 39.
37. D. W. VAN KREVELEN, C. VAN HERDEN and F. J. HUNTJENS, Fuel, 30 (1951) 253.

38. H. H. HOROWITZ and G. METZGER, Anal. Chem., 35 (1963) 1464.
39. J. ZSAKÓ, J. Thermal Anal., 5 (1973) 239.
40. T. OZAWA, Bull. Chem. Soc. Jap., 38 (1965) 1881.
41. G. KRIEN, Proc. 3rd Symp. Chem. Problems Stability Explosives, Ystad, 1973, p. 33.
42. J. H. SHARP and S. A. WENTWORTH, Anal. Chem., 41 (1969) 2060.
43. H. J. BORCHARDT and F. DANIELS, J. Am. Chem. Soc., 79 (1957) 41.
44. A. A. BLUMBERG, J. Phys. Chem., 63 (1959) 1129.
45. H. M. HAUSER and J. E. FIELD, Thermochim. Acta, 27 (1978) 1.
46. E. S. FREEMAN and B. CARROLL, Anal. Chem., 62 (1958) 394.
47. T. OZAWA, J. Thermal Anal., 7 (1975) 601.
48. R. N. ROGERS and E. D. MORRIS, Anal. Chem., 38 (1966) 412.
49. R. G. PATEL and M. M. CHAUDHRI, Thermochim. Acta, 25 (1978) 247.
50. P. K. DÁVID and E. ZELENYÁNSZKI, J. Thermal. Anal., 5 (1973) 337.
51. H. ANDERSON, W. BESCH and D. HABERLAND, ibid., 12 (1977) 59.
52. H. L. FRIEDMANN, J. Macromol. Sci. Chem., 1 (1967) 57.
53. F. ŠKVÁRA, J. ŠESTÁK and V. ŠESTÁK, Op. Cit. Ref., 4 (1974) 105.
54. P. S. NOLAN and H. E. LEMAY, JR., Thermochim. Acta, 6 (1973) 179
55. D. T. Y. CHEN and P. H. FONG, ibid., 18 (1977) 161
56. P. H. FONG and D. T. Y. CHEN, ibid., 18 (1977) 273
57. G. G. T. GUARINI, R. SPINICCI, F. M. CARLINI and D. DONATI, J. Thermal Anal., 5 (1973) 307.
58. J. N. MAYCOCK and V. R. PAI VERNEKER, Thermochim. Acta, 1 (1970) 191.
59. T. ISHII, R. FURUICHI and Y. HARA, J. Thermal Anal., 11 (1977) 71.
60. A. LUCCI and M. TAMANINI, Thermochim. Acta, 13 (1975) 147.
61. E. SEGAL and D. FATU, J. Thermal Anal., 9 (1976) 65.
62. R. G. PATEL and M. M. CHAUDHRI, Proc. 4th Symp. Chem. Problems Stability Explosives, J. Hansson, ed., 1977, p. 347.
63. B. N. N. ACHAR, G. W. BRINDLEY and J. H. SHARP, Proc. Int. Clay Conf., Jerusalem, 1966, p. 67.
64. G. BERTRAND, Synergetics, Springer—Verlag, Berlin, 1979, p. 147.